Does a sex difference of AMPA receptor trafficking after oxygen-glucose deprivation exist in rat cortical and hippocampal slices?

by

Yuyi Xu

A thesis
presented to the University of Waterloo
in fulfillment for the
thesis requirements of the degree of
Master of Science
in
Public Health and Health Systems

Waterloo, Ontario, Canada, 2019

Author's Declaration

I hereby declare that I am the sole author of this thesis. This is a true copy of the thesis, including any required final revisions, as accepted by my examiners.

I understand that my thesis may be made electronically available to the public.

Abstract

Stroke, which is caused by an interruption of blood supply to the brain, is a major public health burden because it is one of the leading global causes of death and disability. AMPA receptor trafficking is considered to play a vital role in the way cells respond to ischemic stroke, but the underlying mechanisms within different brain regions and between male and female tissue are still unclear.

In this study, an acute slice model with a 10 min oxygen-glucose deprivation (OGD) challenge was used to induce dramatic energy and oxygen deprivation and simulate ischemic stroke. A TTC assay was conducted to measure cellular viability after OGD. Surface expression of AMPA receptor subunits, GluA1 and GluA2, was measured under control, or OGD conditions to analyze the pattern of AMPA receptor trafficking. To examine the possible region and sex differences, slices from different brain regions (septal hippocampus vs. temporal hippocampus vs. motor cortex) of each sex were collected. The data were analyzed using a two-way factor, mixed model ANOVA.

According to the TTC assay results, after a 3 h recovery following 10 min OGD, metabolism decreased in all groups, but there was no significant interaction effect between sex and region ($p = 0.84$, $F_{(2,48)} = 0.17$), and no significant main effect of region ($p = 0.34$, $F_{(2,48)} = 1.11$), or sex ($p = 0.62$, $F_{(1,48)} = 0.24$). Similarly, the immunoblot results showed no sex-region interaction (GluA1: $p = 0.41$, $F_{(2,21)} = 0.93$; GluA2: $p = 0.11$, $F_{(2,21)} = 2.40$) and no significant main effect of region (GluA1: $p = 0.91$, $F_{(2,21)} = 0.096$; GluA2: $p = 0.98$, $F_{(2,21)} = 0.020$), or sex

(GluA1: $p = 0.21$, $F_{(1,21)} = 1.71$; GluA2: $p = 0.14$, $F_{(1,21)} = 2.33$), on GluA subunit surface expression after OGD. In addition, based on the calculated effect sizes (partial eta-squared, η_p^2), none of the differences could be regarded as notable ($\eta_p^2 = 0.14$ indicates a large magnitude of effect).

In summary, metabolic function and surface expression of GluA1 and GluA2 were not significantly different between cortical and hippocampal slices, or between male, or female-derived slices, following a 10 min OGD challenge.

Acknowledgements

I am especially indebted to Dr. John G. Mielke, my committee chairman and research supervisor, for his continuous support to my study, for his patience, advice, encouragement, and enthusiasm. I cannot express enough thanks to him for generously providing detailed and valuable guidance for not only the completion of the thesis, but also life and work plan.

Beside my supervisor, I would like to express my sincere appreciation to the rest of my thesis committee, Dr. Joe Tauskela and Dr. Mike Beazely, who have been actively providing me with updated research views and insightful comments. Thank you for broadening my horizon, and providing me opportunities to keep learning new professional knowledge and research skills.

I am also grateful to all my fellow lab mates, Jonathan Thacker, Tony Fong, Sheleza Ahad, Saeideh Davari, and Nicole D'Costa, with whom I have had the pleasure to work and study together.

I thank my friends for supporting and accompanying me when I met difficulties. I would also like to thank my parents and family, whose love and support are always with me, despite the long distance (more than 11,000 km) between us.

Table of contents

List of Figures

List of Tables

List of Abbreviations

ACSF: Artificial Cerebral Spinal Fluid
ANOVA: Analysis of Variance
AMPA: α-amino-3-hydroxy-5-methyl-4-isoxazole propionic acid
ATP: Adenosine Triphosphate
BSA: Albumin
CA1: Cornu Ammonis 1
CA3: Cornu Ammonis 3
CaMKII: Calcium-Calmodulin-Dependent Protein Kinase II
CBF: Cerebral Blood Flow
DALYs: Disability-Adjusted Life Years
DG: Dentate Gyrus
ECL: Electrochemiluminescence
EPSP: Excitatory Postsynaptic Potentials (EPSP)
ERs: Estrogen Receptors
F-HP-S: Female-Hippocampus-Septal
F-HP-T: Female-Hippocampus-Temporal
F-MCx: Female-Motor Cortex
GluA1-4: Glutamate AMPA Receptor 1-4
GluN1-4: Glutamate NMDA Receptor 1-4
HP: Hippocampus
LTD: Long-Term Depression
LTP: Long-Term Potentiation
MCAO: Middle Cerebral Artery Occlusion
MCx: Motor Cortex
M-HP-S: Male-Hippocampus-Septal
M-HP-T: Male-Hippocampus-Temporal
M-MCx: Male-Motor Cortex
NMDA: N-methyl D-aspartate
nNOS: neuronal Nitric Oxide Synthase
NO: Nitrous Oxide
OGD: Oxygen-Glucose Deprivation
PKA: Protein Kinase A
PKC: Protein Kinase C
PVDF: Polyvinylidene Fluoride
rtPA: recombinant tissue Plasminogen Activator
SEM: Standard Error of the Mean
TTC: *2,3,5*-Triphenlytetrazolium chloride

1. Literature Review

Stroke is caused by an interruption of blood supply to the brain. The reduced blood supply dramatically induces energy and oxygen deprivation, which can lead to cell death and severe brain dysfunction. While interruption of blood flow to the brain can be triggered by either a blood clot (ischemic), or a vessel rupture (hemorrhagic), about 87% of strokes are ischemic (American Heart Association, 2017). Notably, the symptoms of stroke, including one-sided motor impairment, aphasia, and hemianopsia (Donnan et al., 2008), usually occur right after the onset of stroke and can be transient, or permanent.

1.1 Public health burden of stroke

Because of its severe consequences, stroke is one of the leading global causes of death and disability. In 2015, an estimated 6.7 million people died from stroke, accounting for 12% of all global deaths (World Health Organization, 2017). In addition, stroke is the second leading global cause of disability, resulting in 5 million people being permanently disabled every year (World Health Organization, 2017). In 2013, 102 million stroke-related disability adjusted life years (DALYs) were estimated to have been lost globally (Feigin et al., 2016). According to an estimate from the World Health Organization (Mendis et al., 2011), the enormous global burden of stroke will likely increase over the following decades in developing countries, and will be a major challenge to public health systems. In Canada, stroke also brings a heavy burden to society and family. According to a prevalence study (Krueger et al., 2015), in 2013, more than 400,000 Canadian patients were struggling with impairments caused by stroke, which costs more than 3.6

billion CAD annually (Ontario Stroke Network, 2016). As a result, understanding the underlying cellular mechanisms of stroke is urgent.

Although stroke can occur at any age, almost three-fourths of strokes occur in people over the age of 65 (Ontario Stroke Network, 2016). Aging is one of the most important risk factors of stroke, and the incidence rate of stroke increases rapidly after the age of 55 (Ontario Stroke Network, 2016). In addition, noticeable sex differences exist in stroke, which is 25% more likely to occur among men (Ontario Stroke Network, 2016; Stroke.nih.gov., 2017). Other risk factors for stroke include hypertension, smoking, obesity, hypercholesterolemia, and previous stroke (Donnan et al., 2008), all of which are highly related to unhealthy diet, low physical activity level, tobacco use, and alcohol intake (World Health Organization, 2017).

1.2 Current treatment and prevention strategies

To relieve the burden of stroke, current clinical practice has shown that rapid treatment of recombinant tissue plasminogen activator (rtPA), such as alteplase, can significantly improve health outcomes after the onset of stroke (National Institute of Neurological Disorders and Stroke rt-PA Stroke Study Group, 1995; Atlantis, 2004; Hacke et al., 2008). However, the consensus on the safe and efficient therapeutic window for stroke is between 3 to 4.5 hours (Atlantis, 2004; Hacke et al., 2008; Paciaroni et al., 2009; Powers et al., 2018). As a result, if stroke occurs, prompt treatment is necessary to minimize brain damage. However, prompt treatment is challenging because a brain scan and other test procedures, such as noninvasive vascular imaging tests, are required to confirm the type of stroke before treatment. According to

the latest guidelines (Powers et al., 2018), brain-imaging tests are recommended to be completed within 20 minutes of patient arrival. For patients who are not suitable for the rtPA treatment, another emerging treatment strategy for stroke is endovascular therapy, which is a microcatheter inserted to remove blood clots and release drugs (Sacks et al., 2013).

As the clinical treatment is highly time dependent, the demand on medical resources is high. To balance the cost and benefit of stroke management, it is also important to include the public health prevention system. Current primary prevention strategies focus on the control of risk factors, such as dietary modification, control of tobacco use, and the administration of prevention drug therapy, such as thrombolysis, to high-risk populations (Donnan et al., 2008). At the same time, to reduce the incidence and severity of recurrent stroke, secondary prevention is designed to be implemented during the recovery period to manage risk factors (Wein et al., 2018). For example, application of thrombolysis, such as aspirin treatment, can reduce the risk of disability after stroke in some conditions (Hackam & Spence, 2007; Wein et al., 2018). Furthermore, stroke rehabilitation, a tertiary strategy, may be applied for stroke recovery. In Canada, every year around 6500 patients are screened for in-patient stroke rehabilitation for a median of 30 days following stroke onset, and then delivered to long-term care through outpatient services (Hebert et al., 2016).

To consummate the current treatment and prevention framework of stroke, further understanding of stroke mechanisms and more evidence-based approaches are needed. According to the guidelines for the prevention of stroke and transient ischemic attack (Kernan et

al., 2014), the benefits of weight loss among patients with an ischemic stroke and obesity are unclear. Also, while the application of prevention treatments, such as statins (Odden et al., 2015) and angiotension receptor antagonists (Chen et al., 2015), are cost-effective for the primary prevention of stroke, the benefits can be counteracted by an increase of geriatric-specific adverse effects, such as muscle-related aches and liver-enzyme abnormalities (Armitage et al., 2019; Schiattarella et al., 2012; Scott et al, 2009). Finally, the average first year inpatient rehabilitation cost from 2001 to 2005 was $17,081 in the US (Godwin et al., 2011), which is a burden to both stroke survivors and health systems. Given currently overwhelmed health systems and limited medical resources, more effective and efficient secondary prevention and treatment strategies are required to cope with stroke and its related brain damage.

1.3 Pathophysiology of ischemic stroke

As about 87% of strokes are ischemic (American Heart Association, 2017), it is vital to understand the pathophysiology of ischemic stroke. Ischemic stroke is induced by the interruption of blood supply, which reduces the energy and oxygen available to the brain. If the deprivation occurs among wide areas of brain, stroke is classified as global ischemia; if the deprivation occurs only in a specified region, it is focal ischemia (Siesjö et al., 1995). Typically, focal ischemia is less severe. Although the ischemic center undergoes irreversible necrosis, the penumbral regions surrounding the occluded artery are potentially salvageable, as biochemical cascades leading to selective cell death can be triggered in this area (Siesjö et al., 1995; Siesjö, 1992; de Lores Arnaiz & Ordieres, 2014).

1.3.1 Ischemic cascade

The ischemic cascade is a series of biochemical events triggered by the onset of ischemia. The brain requires a consistent supply of oxygen and glucose to retain normal function (Mergenthaler et al., 2013; McIlwain et al., 2013). The brain cannot store a large amount of energy, and heavily relies on aerobic metabolism (Mergenthaler et al., 2004), so that, during an ischemic stroke, the brain suffers a rapid decrease of ATP. As a result, the ATP-dependent ion transport pumps fail, and the electrochemical gradients are damaged, which can induce membrane depolarization (Scheiner-Bobis, 2002). The failure of the Na^+/K^+ pump, a crucial ion transporter maintaining a high intracellular K^+ level and a low intracellular Na^+ level, will lead to an increase of intracellular Na^+ and activation of the Na^+/Ca^{2+} exchanger, which will accelerate the accumulation of intracellular Ca^{2+} (de Lores Arnaiz & Ordieres, 2014; ScheinerBobis, 2002). Next, the influx of calcium ions can trigger the release of neurotransmitters, such as glutamate and aspartate, from presynaptic terminals (Weilinger et al., 2013). The increased concentration of extracellular glutamate can lead to the opening of many ionotropic transmembrane receptors, such as N-methyl-D-aspartate (NMDA) receptors and α-amino-3-hydroxy-5-methyl-4-isoxazolepropionic acid (AMPA) receptors (Weilinger et al., 2013; Szydlowska & Tymianski, 2010), which will further induce the influx of calcium ions. The excess internal concentration of calcium ions overactivates a range of cellular signaling pathways and leads to the production of free radicals and calcium-dependent enzymes, which can break down cell membranes and lead to cell death in a process called excitotoxicity (Szydlowska & Tymianski, 2010). As well,

mitochondria, vital organelles regulating cell survival, play an important role in cellular calcium signaling, and impairments of mitochondrial respiration caused by injury can depolarize the mitochondrial membrane potential leading to excessive release of calcium ions and contribute to the cascade of neuronal death after ischemic stroke (Szabadkai & Duchen, 2008; Kirichok et al., 2004).

One possible pathway induced by the influx of calcium ions is the activation of neuronal nitric oxide synthase (NOS), leading to the production of the free radical nitric oxide (NO) (Johnston et al., 2011; Forstermann & Sessa, 2011). NO can form a complex with superoxide, leading to toxic peroxynitrite molecules that can add nitrate to tyrosine groups on proteins and contribute to the production of hydroxyl radicals, which cause lipid peroxidation of proteins and DNA (Johnston et al., 2011; Cherubini et al., 2005). Nitric oxide can also disrupt the function of cytochrome oxidase, and increase production of superoxide and peroxynitrite ions in mitochondria, which is harmful to mitochondrial respiration (Taylor & Moncada, 2010; Johnston et al., 2011). According to another possible pathway, calcium ions entering through NMDA receptors can activate calpain, a protease that can degrade cell structure and induce further apoptosis (Stys & Jiang, 2002). In addition, the activated calpain can also trigger caspase-3 involved apoptosis execution (Schwab et al., 2002; Johnston et al., 2011). Overall, the influx of calcium and release of glutamate will induce various cell signaling events that may lead to cell death.

After focal cerebral ischemia, the cells immediately surrounding the site of blood

interruption usually die through necrosis (Hakim, 1998). The penumbra, however, suffers less serious energy deficiency and experiences milder damage (Hakim, 1998; Broughton et al., 2009; Bonfoco et al., 1995), so that a progressive apoptotic cascade is triggered. The different types of cell death, apoptosis and necrosis, indicate that although the penumbra is also under the threat after ischemia, it is potentially recoverable and thus well worth the exploration of therapeutic intervention (Hakim, 1998; Broughton et al., 2009).

1.3.2 Glutamate receptors

Glutamate is the most important excitatory neurotransmitter in the brain. Glutamate receptors are widely located on postsynaptic membranes, and mediate the vast majority of postsynaptic excitation (Traynelis et al., 2010; Lau & Tymianski, 2010). Glutamate receptors can be divided into ionotropic and metabotropic classes. In recent decades, ionotropic glutamate receptors (iGluRs), such as NMDA receptors and AMPA receptors, have been widely studied (Traynelis et al., 2010; Lau & Tymianski, 2010).

The heterotetrameric NMDA receptor contains two obligatory GluN1 subunits and two GluN2 subunits, each of which has an extracellular N-terminal domain and an intracellular C-terminal domain (Paoletti et al., 2013). Currently, there are four different GluN2 subtypes thought to exist (GluN2A-D) (Lau & Tymianski, 2010). The distribution of the four GluN2 subunits varies, with GluN2A widely distributed in the brain, GluN2B primarily distributed in the forebrain, GluN2C primarily distributed in the cerebellum, and GluN2D primarily distributed in the thalamus (Lau & Tymianski, 2010). In addition, the level of GluN2B is higher in postnatal

brain, but the level of GluN2A exceeds that of GluN2B during development (Johnston et al., 2011). The higher level of GluN2B is thought to be related to the greater learning abilities at childhood (Liu et al., 2004). However, the higher level of GluN2B is also one possible reason for the different vulnerability of brain at different ages, as NMDA channels with a larger portion of GluN2B subunits open more easily and stay open longer (Johnston et al., 2011).

AMPA receptors are formed by four types of subunits, GluA1-4, each of which has an extracellular N-terminus and intracellular C-terminus (Henley & Wilkinson, 2016; Wright & Vissel, 2012). As most AMPA receptors are heteromers containing GluA1/GluA2, or GluA2/GluA3 (Lu et al., 2009), the existence of GluA2 is responsible for regulating excitatory synaptic transmission by controlling the influx of calcium and sodium ions (Man, 2011). The GluA2 subunit inhibits the AMPA receptor's calcium permeability, which helps to maintain the low intracellular calcium concentration at basal conditions in mature neurons, because of the selectively targeted Q/R site editing (Man, 2011; Wright & Vissel, 2012; Whitney et al., 2008). In contrast, the presence of GluA2-lacking AMPA receptors will lead to increasing calcium permeability and further excitotoxicity (Koszegi et al., 2017).

Ischemia is thought to affect GluA2 levels in cultured hippocampal neurons by inducing a rapid endocytosis of GluA2, resulting in a switch to GluA2-lacking calcium permeable AMPA receptors (Blanco-Suarez & Hanley, 2014; Koszegi et al., 2017). The existence of GluA2-lacking calcium permeable AMPA receptors can induce the influx of calcium ions and further plasma membrane injuries (Farber, 1990; Man, 2011; Henley & Wilkinson, 2016; Wang et al., 2012). As

a result, during ischemia, dysregulated GluA2-lacking AMPA receptors can induce excessive calcium influx and cause excitotoxicity (Man, 2011; Henley & Wilkinson, 2016; Wang et al., 2012).

1.3.3 AMPA receptor trafficking

The movement of receptors to, or from, the cell surface is known as receptor trafficking. Receptor trafficking can regulate the density of postsynaptic receptors and adjust the efficiency of response to the release of neurotransmitters (Bedford, 2009). The dynamically regulated GluA2-lacking AMPA receptor distribution is also considered the result of receptor trafficking (Tanaka et al., 2000; Pellegrini-Giampietro et al., 1997). For example, according to neuronal cell culture studies, under basal conditions, most GluA2-lacking AMPA receptors are located at presynaptic sites, or endosomes (Hanley, 2014). When stimulation, such as the influx of calcium ions, is applied, GluA2-lacking AMPA receptors are rapidly expressed at the surface of postsynaptic neurons (Hanley, 2014;). Regulation of this process requires post-translational modifications. Phosphorylation and de-phosphorylation are the most widely studied modifications, and can regulate endocytosis by changing the binding affinity of trafficking adaptors (Bedford, 2009). For example, phosphorylation can increase the interaction of AMPA receptors with scaffolding and cytoskeleton proteins (Derkach et al., 2007). Furthermore, some studies have examined the influence of tyrosine phosphorylation of GluA2 in AMPA receptor trafficking and plasticity. For example, Y876 phosphorylation of GluA2 will downregulate the endocytosis of GluA2 and prevent the internalization of AMPA receptors during long-term

depression (LTD) induction (Lu & Roche, 2012).

Oxygen-glucose deprivation (OGD), which causes excitotoxicity and delayed cell death due to the extracellular accumulation of excessive glutamate (Beattie, 2000), may alter the surface expression of AMPA receptors. In a basal state, the main synaptic AMPA receptors are GluA1/2 and GluA2/3 heteromers (Jaafari et al., 2012). After OGD, however, internalization of GluA2 subunits can be observed in cultured hippocampal neurons, and leads to the increased surface expression of GluA2-lacking, Ca^{2+}-permeable AMPA receptors (Blanco-Suarez & Hanley, 2014; Liu et al., 2006). The GluA2-lacking AMPA receptors allow calcium influx and are essential to OGD-induced cell death in hippocampal neurons (Blanco-Suarez & Hanley, 2014; Liu et al., 2006).

One possible factor regulating the surface expression of AMPA receptors after OGD is the internalization of GluA2-containing AMPA receptors (Beattie, 2000). According to *in vitro* data, administration of excess glutamate can induce rapid internalization of GluA2-containing AMPA receptors (Beattie et al., 2000). After OGD, the initial rapid phase (calcium influx through NMDA receptors) induces GluA2-lacking AMPA receptor insertion, and a later phase reduces GluA2 subunit expression by downregulating its mRNA expression (Malenka, 2003; Hayashi et al., 2000; Blanco-Suarez & Hanley, 2014).

In addition, phosphorylation can directly regulate the electrophysiological, structural, and biochemical properties of AMPA receptors, and is vital for synaptic plasticity (Lu & Roche, 2012; Zhang et al., 2013). The phosphorylation level of AMPA receptors can be altered after

ischemia, and can further affect surface expression of AMPA receptors (Carvalho et al., 2000; Zhang et al., 2013). According to Lu & Roche (2012), subunits can be phosphorylated on tyrosine residue 876 (Y876) by protein kinases such as CaMKII, PKA, and PKC, and the phosphorylation level of the GluA1 subunit in the rat hippocampal CA1 region is increased after ischemia, which may be mediated by activated CaMKII (Fu et al., 2004; Takagi et al., 2003).

1.4 Regional differences in the effect of ischemia

In general, regions with higher demand of energy, or those located in vascular border areas are more vulnerable to injuries like ischemia (Cervos-Navarro & Diemer, 1991). In addition, cellular differences, such as the distribution of glutamate receptors, can influence robustness due to the alteration of calcium ion permeability. According to previous studies, the hippocampus, which plays a vital role in memory formation and spatial awareness (Bannerman et al., 2004), is very sensitive to ischemic injury (Schmidt-Kastner & Freund, 1991). In particular, CA1 pyramidal neurons in the hippocampus are more vulnerable than CA3 pyramidal neurons to brain injury, such as that caused by ischemia (Busl & Greer, 2010; Lalonde & Mielke, 2014; Koszegi et al., 2017). The subfield difference may be mediated by the decrease of synaptic AMPA receptors (e.g., both GluA1 and GluA2) after OGD in CA3 pyramidal neurons, but not in CA1 pyramidal neurons (Dennis et al., 2011).

1.4.1 Differences across the longitudinal axis of the hippocampus

Furthermore, some studies have realized the anatomical and functional differences within the hippocampal structure, along the longitudinal axis (Fanselow & Dong, 2010; Nguyen et al.,

2015; Diniz et al., 2016; Floriou-Servou et al., 2018; Zhang et al., 2018; Gulyaeva, 2018).

Generally, the septal (or dorsal) and temporal (or ventral) poles are regarded as two distinct

regions with different physiologic functions (Bekiari et al., 2015). The septal pole is thought to

be more linked to cognitive functions (Moser et al., 1995), whereas the temporal pole is thought

to be more related to the regulation of stress and emotion (Henke, 1990; Fanselow & Dong,

2010).

Since the 1980s, different brain injury levels between the septal and temporal poles within

the hippocampus after ischemia have been noticed (Smith et al., 1984; Ashton et al., 1989).

Some studies have shown that the CA1 region in the septal pole is more vulnerable to ischemia

than the same region in the temporal pole (Ashton et al., 1989). One possible reason may be the

high cerebral blood flow (CBF) in the temporal CA1 region (Ashton et al., 1989). In addition, the

septal CA1 region contains a higher density of pyramidal neurons, which may reduce the

glia/neuron ratio and lead to higher susceptibility to ischemia (Ashton et al., 1989).

However, some studies have reached a different conclusion. For example, it was observed

from electrophysiological data that neurons in the temporal pole were intrinsically more

excitable than those in the septal pole (Papatheodoropoulos & Kostopoulos, 2000; Dougherty et

al., 2012). According to Papatheodoropoulos and Kostopoulos (2000), increasing calcium ions

from a basal level to 5 mM induced an enhancement of baseline CA1 field excitatory

postsynaptic potentials (EPSP) only in temporal hippocampal slices, which indicates that the

temporal hippocampus is more excitable and has a higher neurotransmitter release probability. In

addition, Onufriev et al. (2017) found that after ischemia, corticosterone was released in the temporal pole, but not in the septal pole, which indicates the possibility of different neuroinflammation mechanisms between the two regions. As a result, it is likely that the vulnerability to OGD varies along the longitudinal axis (Rami et al., 1997; Czerniawski et al., 2009; Fanselow and Dong, 2010; Isaeva et al., 2015; Strange et al., 2014; Bekiari et al., 2015; Floriou-Servou et al., 2018), but the phenomenon and potential mechanisms are not fully understood.

1.4.2 Differences between hippocampus and cortex

Cortical neurons (Blanco-Suarez & Hanley, 2014; Schmidt-Kastner & Freund, 1991), which affect musculoskeletal control, perception, memory, cognition, awareness, language, and consciousness (Siegelbaum & Hudspeth, 2000), appear to be more robust to ischemic injury than hippocampal neurons (Blanco-Suarez & Hanley, 2014). An *in vivo* rat acute hypoxia experiment showed that the mitochondrial respiratory rate decreased in hippocampal mitochondria, but not in cortical mitochondria due to differences in NO metabolism and membrane potential change patterns (Czerniczyniec et al., 2015). In addition, evidence also suggests that the regional differences may be caused by different AMPA receptor trafficking patterns. Work done with neuronal cultures after OGD (Blanco-Suarez & Hanley, 2014; Koszegi et al, 2017) shows that rapid internalization of the GluA2 subunit exists in hippocampal neurons, but not in cortical neurons, which may be mediated by the hippocampal specific PICK1-dependent synaptic expression of GluA2-lacking AMPA receptors (Koszegi et al, 2017; Jaafari et al., 2012).

1.5 Sex differences in ischemia

The presence and potential mechanism of sex differences after OGD have been well discussed in recent decades. The incidence of clinical stroke is higher in men until 85 years of age (Manwani and McCullough, 2011). Generally, male brain is thought to be more vulnerable to ischemia than female brain in both animal and clinical studies (Reeves et al., 2008; Liu et al., 2009; Cheng and Hurn, 2010; Manwani and McCullough, 2011). The sex difference is usually thought to be related to the effects of hormones, but hormone-independent intrinsic factors have been discussed in recent decades as well (Gibson, 2013).

Generally, the effects of estrogens are considered neuroprotective (Manwani & McCullough, 2011). Female rats were observed to have a more severe infarct and higher cognitive impairments after the removal of ovaries (Cai et al., 2014), and this effect could be reversed by the supplement of exogenous estrogen in middle-aged female rats (De Butte-Smith et al., 2009). One possible beneficial effect of estrogen may be the estrogen receptor (ER) mediated inhibition of NADPH oxidase, which can reduce the ischemic damage (Zhang et al, 2009). In addition, some studies have revealed that the distribution of ERs varies along the longitudinal axis of the hippocampus, with more ERs within GABAergic neurons in the septal pole, which may cause different neuroprotective effects between septal and temporal hippocampus (Hart et al., 2001).

The effect of testosterone is still controversial, and tends to be dose- and age- dependent (Uchida et al., 2009; Kim & Vemuganti, 2015). Some experiments have revealed that testosterone supplements can worsen infarct size after ischemia by regulating transcription of

inflammatory genes (Cheng et al., 2007; Hawk et al. et al., 1998), however, other studies have indicated that testosterone application can be neuroprotective by relieving oxidative stress (Ahlbom et al., 2001; Fanaei et al., 2014). A possible explanation of the dimorphic effect was revealed by a study (Uchida et al., 2009) indicating that low doses of testosterone can help mice brain recover after ischemia, but high doses of testosterone can cause an inverse effect.

Importantly, hormones cannot fully explain the sexually dimorphic patterns after ischemia, as sex differences also exist among preadolescents and the elderly (Du et al., 2004; Gibson, 2013). Intrinsic factors other than hormones, such as sex chromosomes, may be relevant. According to one cell viability study using cultured neurons, XY neurons after excitotoxicity are more sensitive than XX neurons, because of the inability of XY neurons to maintain intracellular levels of glutathione (a substance that can reverse excitotoxic brain injury) (Du et al., 2004). Some other sex-dependent molecule alterations involved in post-ischemia cell death are also found to not be influenced by hormone changes (Gibson, 2013). For example, neuronal nitric oxide synthase (nNOS), which regulates cell death after ischemia, is male toxic and female protective, by increasing infarction in male mice, but protecting female mice after middle cerebral artery occlusion (MCAO) (McCullough et al, 2005). However, the dimorphic effect of nNOS cannot be influenced by changing hormone exposure (Gibson, 2013).

2. Study Rationale

As regional differences after ischemia have been examined in cultured neurons (Blanco-Suarez & Hanley, 2014), but not in tissue slices, the study aimed to explore the effect of an established *in vitro* model of ischemia (OGD, oxygen-glucose deprivation) on tissue slices prepared from rat hippocampus and motor cortex. In addition, possible sex differences after ischemia were examined in this model by using tissue slices from both male and female rats. Lastly, variability in OGD-mediated AMPA receptor trafficking was explored by comparing the surface expression of GluA2-lacking AMPA receptors across slices from each condition.

In this study, I expected to answer the following questions:

1. Does brain region affect outcome in our OGD model? In particular, are hippocampal slices more vulnerable to OGD than cortical slices, and, within the hippocampus, is the septal pole more vulnerable to OGD than the temporal pole?

2. Does a sex difference exist in our OGD model? Specifically, do male and female brain slices react differently to OGD?

3. Does OGD alter the surface expression of GluA2? If so, is there a difference in OGD-mediated trafficking as a function of either brain region, or animal sex?

Given what has been reported in the literature, brain region and sex were expected to influence slice viability (Cervos-Navarro & Diemer, 1991; Fanselow & Dong, 2010; Gibson, 2013; Lalonde & Mielke, 2014; Kim & Vemuganti, 2015; Floriou-Servou et al., 2018). Based on

the literature and previous work from our laboratory, sexual dimorphism was expected, and male slices were hypothesized to be more sensitive to OGD. Furthermore, different regions of the rat brain were expected to react differently after OGD. Specifically, the hippocampal slices were expected to be more vulnerable than motor cortex slices, and within the hippocampus, the septal pole slices were expected to be more vulnerable than the temporal pole slices. Along with these regional and sex differences in viability, the surface expression of GluA2 was expected to decrease in a manner that paralleled slice viability.

To examine slice viability after OGD, a *2,3,5-* Triphenyltetrazolium Chloride (TTC) Assay was used to measure mitochondrial function (Lalonde & Mielke, 2014). In addition, to determine GluA2 surface expression among the different sample groups, Sulfo-NHS-SS-biotin (Blanco-Suarez & Hanley, 2014) was used to label surface expressed proteins, and the amount of targeted surface GluA2 subunits was identified with SDS-PAGE and immunoblotting.

3. Methods

3.1 Animals

All experiments followed procedures approved by the animal care committee at the University of Waterloo. Male and female, non-sibling Sprague-Dawley rats (weight 250-350 g) were received as young adults and housed in polypropylene cages with woodchip bedding and stainless steel wire lids. Animals were allowed free access to water and standard rodent chow (Teklad rodent diet) and were kept on a 12-hour dark/light cycle in groups of 3 rats per cage.

3.2 Dissection and slice preparation

Before dissection, each rat was anaesthetized in a CO_2 induction chamber and then decapitated. Brains were then quickly extracted and placed in 4°C oxygen-rich (95% O_2: 5% CO_2) artificial cerebrospinal fluid (ACSF; composed of 127.0 mM NaCl, 2.0 mM KCl, 1.2 mM KH_2PO_4, 26.0 mM $NaHCO_3$, 2.0 mM $MgSO_4$, 2.0 mM $CaCl_2$, 10.0 mM glucose; pH 7.37-7.43; 300-320 mOsm; reagents purchased from Sigma Aldrich Canada Co.).

To collect samples for the TTC assay (see section 3.4), or biotinylation (see section 3.5), both hippocampus and motor cortex slices were needed. After dissection, to collect slices from motor cortex, a whole brain mould (Ted Pella, Inc., Redding, CA, USA) for adult rats was used (Thacker et al., 2019). The mould was submerged in chilled ACSF. A razor blade was then placed at position 6 to remove the prefrontal cortex. Next, a mid-sagittal cut was made to separate the hemispheres. To collect hippocampal slices, the hippocampus from the right hemisphere was extracted in a Petri dish filled with chilled ACSF, and tissue slices (350 μm)

were prepared with a McIlwain tissue chopper (Mickle Laboratory Engineering Co., Surrey, UK). From each hippocampus, six septal slices were collected, two intermediate slices were discarded, and six temporal slices were collected. The first, third, and fifth hippocampal slices were assigned to the control group and the second, fourth, and sixth slices were assigned to the OGD group (Figure 7.1 A; Figure 7.1 B; Figure 7.2). The left hemisphere was assigned to be sectioned coronally with a McIlwain tissue chopper to provide six motor cortex slices (350 μm), including the area encompassed by plates 9-21 in the Paxinos and Watson atlas (Paxinos and Watson, 2017; Thacker et al., 2019; Figure 7.1 C; Figure 7.2), with the same assignment rule for the control and OGD groups.

3.3 The OGD model

All slices were placed on inserts containing a semi-permeable membrane, and held at interface in an incubation chamber with oxygen-rich ACSF (35°C ± 0.5°C) for 90 min after slicing. Inserts containing the OGD group slices were transferred to a 35°C ± 0.5°C oxygen-glucose deprivation environment for 10 min (Lalonde & Mielke, 2014). To ensure oxygen-glucose deprivation, the 10 mM glucose in the normal ACSF was replaced by 10 mM sucrose and the solution was gassed with nitrogen (N_2) in a 35°C water bath for at least 60 min prior to use. To control for any stress introduced by the manipulation, the control group slices underwent a SHAM procedure in which they were moved within the chamber containing normal ACSF. After the 10 min OGD challenge, or SHAM procedure, all slices intended for the TTC assay were maintained in a 35°C ± 0.5°C oxygen-rich ACSF environment for a 3-hour recovery

period, and all slices intended for the biotinylation assay were immediately processed (Figure 7.3).

3.4 TTC assay

The *2,3,5-* triphenyltetrazolium chloride (TTC) assay can be used to distinguish cellular metabolic activity levels because the dehydrogenases in metabolically active cells can reduce colorless TTC into a deep red *1,3,5-* triphenylformazan (TPF) (Preston & Webster, 2000; Lalonde & Mielke, 2014). As a result, the TTC assay was performed for each set of slices to test metabolic activity. After a 3-hour recovery from OGD, or SHAM, each group of slices was incubated with 2 mL 2% (w/v) TTC solution (*2,3,5-* TTC powder freshly dissolved in ACSF, gassed with N_2 for 5 min) for 1 h at 35°C ± 0.5°C, under lucifugal conditions. Next, slices were rinsed twice with ACSF that had been gassed with N_2, the metabolites were extracted with 1.5 mL extraction buffer (DMSO: 95% EtOH = 1:1) overnight, and the absorbance was detected at 485 nm with a spectrophotometer (Figure 7.3).

3.5 Biotinylation

Biotinylation is a method to study surface expression and trafficking of receptors (Blanco-Suarez & Hanley, 2014). After the 10 min OGD challenge, 100 μL 10 mM Sulfo-NHS-SS-Biotin (dissolved in chilled ASCF) was separately applied to each tissue slice for 45 min at 4°C in darkness to allow for interaction with surface proteins. After 3 rinses with quenching buffer (TBS; 25 mM Tris, 0.15M sodium chloride; pH 7.2), excess biotin was washed away, and the surface portion labeled by biotin was ready for the protein assay and bead

conjugation (Figure 7.3; Figure 7.4).

3.6 Protein assay

After biotinylation, to collect samples for the immunoblotting experiments, each group of slices was transferred to a 2 mL glass homogenizing tube with 350 µL of chilled non-ionising lysis buffer (composed of 100 mM NaCl, 25 mM EDTA, 10 mM Tris, 1% (v/v) Triton X-100, 1% (v/v) IGEPAL CA-630), supplemented with sodium orthovanadate and a protease inhibitor cocktail (AEBSF, Aprotinin, Bestatin hydrochloride, E-64, Leupeptin hemisulfate salt, Pepstatin A). The slices were manually homogenized with a PTFE pestle and then centrifuged at $1000 \times g$ for 10 min at 4°C. Supernatants were collected for future immunoblot analysis.

Before being stored at -80°C, the concentration of each sample was measured by a DC protein assay kit (BioRad Laboratories, Inc., CA, USA). A linear standard set was freshly prepared with albumin (BSA) dissolved in non-ionising lysis buffer. The standard concentration gradient was typically 0, 0.25, 0.5, 1, 1.25, 1.5, 1.75, 2 µg/µL. The freshly prepared linear BSA standards, as well as each sample were placed into a 96-well plate in triplicate to complete reactions with reagent A' (composed of 20 µL reagent S and 1000 µL reagent A) and reagent B from the kit, so that the optical density of each unknown sample group could be measured and averaged by spectrophotometry (at 750 nm).

3.7 SDS-PAGE and immunoblot analysis

Before conducting SDS-PAGE, 80 µL of Neutravidin beads were washed three times with 500 µL of non-ionising lysis buffer and then incubated with each sample group to target

biotin-labeled surface proteins. After a 4 h incubation with 100 μg total protein sample at 4°C on a rotator, the mixtures were spun and washed three times with 500 μL of non-ionising lysis buffer; after each wash, samples were spun at 10,000 × g for 30 s at 4°C. The sediment, with the bead-biotin-protein complexes, contained the surface proteins needed for further electrophoresis and immunoblot analysis (Figure 7.3).

SDS-PAGE was applied to separate the protein samples based on molecular weight. For protein separation, 10-well 10% gels were freshly prepared. All samples were prepared with 1× sample buffer (composed of 34.9 mM Tris-HCl (pH 6.8), 13.15% (w/v) glycerol, 1.05% SDS, 0.005% bromophenol blue), and were heated at 95°C for 5 min. The samples were separated in running buffer (composed of 3.0 g/L Tris base, 14.4 g/L glycine, and 1.0 g/L of SDS; pH 8.3) at 220 V for 1 h, and were then wet-transferred onto polyvinylidene fluoride (PVDF) membranes in transfer buffer (composed of 25 mM Tris, 192 mM glycine, 20% (v/v) methanol; pH 8.3) at 350 mA, 4°C for 2 h. Each sample was run in duplicate and averaged for statistical analysis later. A Ponceau S image (which revealed the total amount of protein present in each lane of the blot) was used as a confirmation of successful transfer and an internal control for loading variability (Thacker et al., 2016).

Before application of antibodies, membranes were blocked with 5% milk (w/v) made in chilled TBST (composed of 20 mM Tris, 140 mM NaCl, 01% (v/v) Tween-20; pH 7.6) for 1 h. The level of target proteins was detected with corresponding primary and secondary antibodies. The blots were then incubated with primary antibody overnight at 4°C, and then with secondary

antibody for 1 h at room temperature. The GluA1 (rabbit, in 5% milk, 1:1,000, Cell Signaling, Danvers, MA, USA) and GluA2 (rabbit, in 5% milk, 1:1,000, Cell Signaling, Danvers, MA, USA) primary antibodies were tested and compared among different conditions. The corresponding secondary antibody was anti-rabbit (1:2,500, in 5% milk, IgG, Cell Signaling, Danvers, MA, USA). The antibody combinations were detected by digital camera with electrochemiluminescence (ECL) from Crescendo (Immobilon Crescendo western HRP substrate; Millipore).

3.8. Statistical analysis

3.8.1 Software

All data were stored in Microsoft Excel worksheets and analyzed by GraphPad Prism (Verision 6.00) and R (Version 3.1.1). All the images were generated by GraphPad Prism (Verision 6.00) and the statistical significance was set at $p \leqslant 0.05$.

3.8.2 Data exclusion criteria

Before statistical analysis, outliers were identified and excluded from the data set via Tukey's rule (Mosteller & Tukey, 1977), which is not dependent on normality assumptions and less affected by extreme data. The outliers were identified based on the quartiles of the data. The distance between lower quartiles (Q_1) and upper quartiles (Q_3) was the inter quartile range (IQR). Any data point falling out of the range [$Q_1 - 1.5$ IQR, $Q_3 + 1.5$ IQR] was generally treated as a possible outlier, and any data point falling out of the range [$Q_1 - 3$ IQR, $Q_3 + 3$ IQR] was treated as a probable outlier. In this study, only probable outliers were excluded from the data set.

In addition, as the slices exposed to OGD were expected to undergo more severe biological damage than SHAM slices, any TTC experiments where OGD slices showed formazan absorbance higher, or equal to that of the associated control group were excluded from the final data set. Notably, if a data point for one of the three regions was removed, data points for the corresponding regions were also removed (to ensure that only complete sets were used). As a result of the previous *a priori* criteria, 3 of 12 male rats and 2 of 11 female rats were excluded from TTC assay results.

3.8.3 Test for homogeneity of variances and normality

To analyze effects among different groups, analysis of variance (ANOVA) is widely used. However, there are three assumptions that should be met before conducting an ANOVA. The first precondition is the independence of each sample group. Although slices from the three regions (septal hippocampus, temporal hippocampus, and motor cortex) were all prepared from the same rat brain, they were treated and tested separately, so the responses to OGD across the groups can be assumed to be independent. The other two preconditions are homogeneity of variance and the normality of the sample distribution. In our experiments, both the homogeneity of variance and the normality of distribution were tested before we assumed that the sample data met all the preconditions.

Homogeneity of variance was tested to confirm that the expectation of random errors was equal to 0 (variances of each sample group were equal), so that the sample from each different group was statistically comparable. In this study, the Fligner-Killeen test was applied to test the

homogeneity of variances among different groups since the approach is a non-parametric test that doesn't require the normal distribution assumption (Conover et al., 1981). If the result rejects the assumption of homogeneity of variances, transformations (such as logarithmic transformation, square root transformation, and reciprocal transformation) can be applied to adjust the homogeneity of variances, or a non-parametric test can be selected as an alternative to ANOVA.

The normality of the sample distribution was also tested. As the sample size was small and the distribution of measures was unknown, the Shapiro-Wilk normality test (D'agostino et al., 1990; Ghasemi & Zahediasl, 2012), which is ideal for small sample size ($3 < N < 50$), was conducted as the test for normality. To further assess the normality, graphical assessment (Q-Q plot) and an examination of the skewness and kurtosis were applied as well. If the data were normally distributed, the points in the Q-Q plot would lie on a straight diagonal line. Moreover, skewness close to zero indicated symmetry of the distribution. In general: (a) if skewness was less than -1 or greater than 1, the distribution was highly skewed, (b) if skewness was between -1 and -0.5 or between 0.5 and 1, the distribution was moderately skewed, and (c) if skewness was between -0.5 and 0.5, the distribution was approximately symmetric. Similarly, kurtosis is another indicator about the height and sharpness of the central peak. In particular, kurtosis close to 0 indicated a normal distribution, kurtosis larger than 0 indicated a sharp peak, and kurtosis less than 0 indicated a flat peak to the distribution.

3.8.4 Two-way, mixed model ANOVA

Since the tests described in the previous section supported that we could generally assume homogeneity of variance and normality of our sample distributions, the decision was made to select a parametric test to examine the differences among groups after OGD. In this study, the degree to which differences in OGD response were affected by two factors (sex and region) was uncertain In addition, one of the factors, region, consisted of measures from three brain areas (septal hippocampus, temporal hippocampus, and motor cortex) of each animal. As a result, a two-way, mixed ANOVA (with sex as the between subjects factor and region as the within subjects factor) was used to analyze the results.

When evaluating the results, the possible interaction effects between sex and region were first considered. If the $p < 0.05$, there was an interaction, which could be further classified as ordinal (e.g., group means of one sex were always greater than the other sex among all regions), or disordinal (e.g., two, or more group means switched, or crossed). When the data showed no significant interaction ($p > 0.05$), the potential main effects of sex and region were analyzed.

3.8.5 Effect size calculation

To quantify the strength of observed differences, an effect size was calculated as appropriate. Typically, eta-squared (η^2) is widely used for effect size calculation for ANOVA. In addition, if repeated measures and/or multiple factors are involved, partial eta-squared (η_p^2) can be used to better explain the effect from multiple variables (Lakens, 2013).

In particular, $\eta_p^2 = 0.01$ indicates a small magnitude of effect, $\eta_p^2 = 0.06$ indicates a

moderate magnitude of effect, and $\eta_p^2 = 0.14$ indicates a large magnitude of effect. The η_p^2 was

defined as the ratio of variance of an effect over that of the effect and the associated error

variance，based on the following equation:

$$\eta_p^2 = \frac{SS_{effect}}{SS_{effect} + SS_{error}}$$

Where

$SS_{effect} = sum\ of\ square\ for\ the\ effect\ of\ interest;$

$SS_{error} = sum\ of\ square\ for\ the\ error\ term\ associated\ with\ that\ effect.$

4. Results

4.1 TTC assay

4.1.1 Outliers

Any TTC experiments where OGD slices showed formazan absorbance higher, or equal to that of the associated control group were excluded from the final data set. Based on the first criterion, 3 male rats and 2 female rats were excluded. In addition, data points for the corresponding regions were also removed to ensure that only complete data sets were used.

Next, Tukey's method was applied to identify probable outliers in the TTC assay dataset. Any data beyond the fences [Q_1-3 IQR, Q_3+3 IQR] of each group were removed from the data set. As noted in Table 7.1, there were no values beyond the fences. As a result, 9 of 12 male rats and 9 of 11 female rats were selected as the data set for further TTC assay analysis.

4.1.2 Homogeneity of variances and normality

The TTC results were tested for homogeneity of variances and normality of distribution (Table 7.2). In this dataset, the Fligner-Killeen test for homogeneity of variances was applied, and the interaction of multiple variables (e.g., sex, and region) was considered to adjust the degrees of freedom. The result ($p = 0.21$) showed no significant difference between the variances among the groups, so the TTC assay results were taken to have met the assumption of homogeneity of variance.

Furthermore, the normality of the sampling distribution was tested (Table 7.2). In this study, the Shapiro-Wilk test was applied, as it is relatively optimal for small sample sizes ($3 < N < 50$).

All 6 groups, which were divided by sex and region (M-HP-S, M-HP-T, M-MCx, F-HP-S, F-HP-T, and F-MCx), were compared. In 4 of 6 groups, the null hypothesis regarding normality could not be rejected ($p > 0.05$, respectively), the remaining two groups (male temporal hippocampus ($p = 0.04$), and female septal hippocampus ($p = 0.04$), however, may not follow a normal distribution. Although different transformation methods could be used to adjust the raw data before further analysis, since the p values were close to the 0.05 threshold the assumption could be made that the departure from normality was not excessive.

To further assess normality, graphical assessment (Q-Q plot) and an examination of the skewness and kurtosis were applied. If the data were normally distributed, the points in a Q-Q plot would lie on a straight diagonal line. According to Figure 7.5, besides the Q-Q plots of male temporal hippocampus and female septal hippocampus, all others resembled a straight line, which parallels the Shapiro-Wilk test results.

Moreover, skewness and kurtosis were assessed. In general, if skewness was less than -1, or greater than 1, the distribution was highly skewed. The skewness value of the female septal hippocampus group (-1.093) indicated that the distribution might be right skewed (Table 7.2). Kurtosis describes the height and sharpness of the central peak; in particular, kurtosis close to 0 indicates a normal distribution. The most extreme kurtosis value (-1.959) was found for the male temporal hippocampus group, and indicated that the distribution curve might be relatively flat.

The assessment tests indicated that the variances of the TTC data were homogeneous, and that, with the exception of the male temporal hippocampus and female septal hippocampus

groups, the TTC data could be assumed to have followed a normal distribution. Lastly, the data from the different slice groups (M-HP-S, M-HP-T, M-MCx, F-HP-S, F-HP-T, and F-MCx) were treated as independent samples. Given that linear models are able to withstand modest deviations from normality (Khan & Rayner, 2003), the decision was made to apply a two-way, mixed model ANOVA to analyze the TTC assay data.

4.1.3 TTC metabolism in the OGD model

According to Figure 7.8A, the slice preparation protocol induced little injury to the slices. After a 3-hour reperfusion, the control slices were very clearly metabolically active. In contrast, the 10 min OGD challenge significantly interfered with mitochondrial function to varying degrees.

4.1.4 Region and sex differences in the TTC assay after OGD challenge

To evaluate region and sex-based differences, the formazan absorbance values of OGD groups were taken as a percent of the corresponding control groups. According to the TTC assay, after a 3 h recovery following 10 min OGD, the male septal hippocampus, temporal hippocampus, and motor cortex slices underwent declines of 53.2%, 43.2%, and 51.9% in metabolism, and the female septal hippocampus, temporal hippocampus, and motor cortex slices underwent declines of 59.2%, 57.2%, and 38.1% in metabolism (Table 7.2; Figure 7.8).

In this study, sex was a between-subjects variable, and region was a within-subjects variable (i.e., a repeated, or matched measure); as well, the interaction between sex and region were considered. According to Figure 7.8B and Table 7.3, there was not a significant interaction

between sex and region ($p = 0.84$, $F_{(2,48)} = 0.17$).

Although examining the means alone would suggest that the septal hippocampal slices seemed to be the most vulnerable in both male and female rats, there was no significant main effect of region ($p = 0.34$, $F_{(2,48)} = 1.11$) (Figure 7.8C; Table 7.3). While the male and female slices appeared to differ in their vulnerability, there was no significant main effect of sex ($p = 0.62$, $F_{(1,48)} = 0.24$) (Figure 7.8D; Table 7.3).

4.1.5 Magnitude of the differences

In order to evaluate the magnitude of the observed differences, effect sizes (η_p^2) were calculated. In particular, $\eta_p^2 = 0.01$ indicates a small magnitude of effect, $\eta_p^2 = 0.06$ indicates a moderate magnitude of effect, and $\eta_p^2 = 0.14$ indicates a large magnitude of effect. Based on the results (Table 7.3), the magnitude of the sex difference was very small ($\eta_p^2 = 0.002 < 0.01$), and the magnitude of the regional difference was between small and medium ($0.01 < \eta_p^2 = 0.04 < 0.06$). In addition, the strength of the interaction effect between sex and region was of a medium magnitude ($\eta_p^2 = 0.06$) (Table 7.3).

4.2 Immunoblot analysis

4.2.1 Outliers

In this study, 5 male and 5 female rats were used to analyze surface expression of GluA1 and GluA2 subunits. As with the TTC data, Tukey's method was applied to identify probable outliers. Any data beyond the fences [Q_1 - 3 IQR, Q_3 + 3 IQR] of each group were considered outliers. According to Table 7.4 and Table 7.7, there were 5 extreme values beyond the fences.

Common methods to deal with the outliers, but not to influence sample size, include assigning new estimated values (e.g., the mean value for the rest of the observations, or predicted values by a regression model), or trying a transformation (e.g., log-transform, or square-root transform) (Khan & Rayner, 2003; Cousineau & Chartier, 2010; Bakker & Wicherts, 2014; Kwak & Kim, 2017; Pollet & Meij, 2017). However, as ANOVA is relatively robust to violations of normality (Khan & Rayner, 2003), a two-way, mixed model ANOVA was used for data analysis without the removal of outliers.

4.2.2 Homogeneity of variances and normality

According to the immunoblot results, the optical density of surfaced expressed GluA1 and GluA2 were detected and analyzed, and specifically, the optical density of OGD groups was taken as a percent of the corresponding control groups. The Fligner-Killeen test showed no significant differences among the variances of the different groups for the surface expression of both GluA1 ($p = 0.68$, Table 7.5) and GluA2 ($p = 0.52$, Table 7.8), which indicated that the immunoblot results met the assumption of homogeneity of variance.

Furthermore, the normality of the distribution was tested. The Shapiro-Wilk test was applied, and p-values in all groups were larger than 0.05, except in male temporal hippocampus group ($p = 0.006$ for GluA1, and $p = 0.006$ for GluA2, Tables 7.5 and 7.8). If $p > 0.05$, the null hypothesis could not be rejected, indicating the immunoblot results followed a normal distribution. If $p < 0.05$, the null hypothesis should be rejected. However, as discussed above, ANOVA is relatively robust to violations of the normality assumption, and may still be applied

even if not all data follow a normal distribution.

To further assess the normality, graphical assessment (Q-Q plot) and an examination of the skewness and kurtosis were applied as well. As noted previously, if the data were normally distributed, the points in a Q-Q plot would lie on a straight diagonal line. According to Figure 7.6 and Figure 7.7, although the sample size is relatively small ($N = 5$), all Q-Q plots demonstrated patterns similar to a straight line, which tended to indicate normal distribution.

Moreover, skewness close to zero indicated symmetry of the distribution. According to the GluA1 (Table 7.5) and GluA2 (Table 7.8) immunoblot results, the skewness value indicated that the distribution of all groups might be skewed to varying degrees. Kurtosis is another indicator about the height and sharpness of the central peak. In particular, kurtosis close to 0 indicates a normal distribution, kurtosis larger than 0 indicates a sharp peak, and kurtosis less than 0 indicates a flat peak of distribution. According to the immunoblot results for GluA1 (Table 7.5), the kurtosis values indicated that the distribution curve might be relatively sharp in all groups except the female motor cortex group (-0.792). According to the immunoblot results for GluA2 (Table 7.8), the kurtosis values indicated that the distribution curve might be relatively sharp in all groups except the female temporal hippocampus group (-0.833).

In summary, since the diagnostic tests indicated that both the GluA1 and GluA2 immunoblot data tended to follow a normal distribution and the variances were homogeneous, a two-way, mixed model ANOVA (with sex as the between subjects variable) was applied to analyze the data.

4.2.3 GluA1 surface expression after OGD challenge

According to the immunoblot data of male rats, the surface expression of GluA1 underwent a 43.9% increase in septal hippocampal slices, a 13.5% decrease in temporal hippocampal slices, and a 4.2% decrease in motor cortex slices (Figure 7.9). In contrast, the female data showed a 32.2%, 20.9%, and 0.4% increase of GluA1 surface expression in septal, temporal hippocampus, and motor cortex slices, respectively (Figure 7.9).

To determine the presence of regional and sex differences in GluA1 surface expression after OGD challenge, a two-way, mixed model ANOVA was conducted. Although it seemed that disordinal interaction effect might exist between sex and region (Figure 7.9B), the interaction effect was not significant ($p = 0.41$, $F_{(2,21)} = 0.934$), and there was no significant effect of either region ($p = 0.91$, $F_{(2,21)} = 0.096$), or sex ($p = 0.21$, $F_{(1,21)} = 1.71$) on GluA1 surface expression after 10 min OGD. The data indicated that OGD-mediated changes in GluA1 surface expression of male and female rats were not significantly different among the regions examined after OGD (Table 7.6; Figure 7.9).

4.2.4 Region and sex difference of GluA2 surface expression after OGD challenge

According to the immunoblot data, within the septal hippocampus, OGD caused the surface expression of GluA2 to undergo a 15.1% increase in male rats, and a 51.3% increase in female rats. In contrast, GluA2 surface expression decreased 9.5% in male temporal slices, but increased 23.1% in female temporal slices. In motor cortex, GluA2 surface expression decreased more in male (15.6%) than female (4.0%) slices (Figure 7.10).

To examine regional and sex differences in GluA2 surface expression after 10 min of OGD, a two-way, mixed model ANOVA was conducted (Table 7.9; Figure 7.10). In this study, there was no significant interaction between sex and region ($p = 0.11$, $F_{(2,21)} = 2.40$). In addition, there was no significant effect of either region ($p = 0.98$, $F_{(2,21)} = 0.020$), or sex ($p = 0.14$, $F_{(1,21)} = 2.33$) on GluA2 surface expression after 10 min OGD. The data indicated that OGD-mediated changes in GluA2 surface expression of male and female rats were not significantly different among the regions examined after OGD (Table 7.9; Figure 7.10).

4.2.5 Magnitude of the differences

In order to evaluate the magnitude of the observed differences, effect sizes (η_p^2) were calculated. As noted, $\eta_p^2 = 0.01$ indicates small magnitude of effect, $\eta_p^2 = 0.06$ indicates moderate magnitude of effect, and $\eta_p^2 = 0.14$ indicates large magnitude of effect. Based on the GluA1 results (Table 7.6), the magnitude of the sex difference was small ($\eta_p^2 = 0.015$), and the magnitude of the regional difference was between small and medium ($0.01 < \eta_p^2 = 0.043 < 0.06$). In addition, the strength of the interaction effect between sex and region ($0.06 < \eta_p^2 = 0.081 < 0.14$) was calculated as well, and was observed to have a medium to large magnitude.

Similarly, the magnitude of sex and regional differences of GluA2 surface expression alteration were calculated (Table 7.9). The magnitude of the sex difference was medium to large ($0.06 < \eta_p^2 = 0.088 < 0.14$), and the magnitude of the regional difference was between small and medium ($0.01 < \eta_p^2 = 0.026 < 0.06$). In addition, the strength of the interaction effect between sex and region ($0.01 < \eta_p^2 = 0.044 < 0.06$) was small to medium.

5. Discussion

In this study, the effect of an established *in vitro* model of ischemia (OGD, oxygen-glucose deprivation) on tissue slices prepared from rat hippocampus and motor cortex was examined. In addition, possible sex differences after ischemia were examined by using tissue slices from both male and female rats. A *2,3,5*- Triphenyltetrazolium Chloride (TTC) Assay was used to measure mitochondrial function for slice viability comparisons (Lalonde & Mielke, 2014). In addition, Sulfo-NHS-SS-biotin (Blanco-Suarez & Hanley, 2014) was used to label surface expressed proteins, and the amount of targeted surface GluA1 and GluA2 subunits was identified with SDS-PAGE and immunoblotting to determine GluA1 and GluA2 surface expression among the different sample groups.

According to the TTC assay data, although it was hypothesized that the hippocampal slices would be more vulnerable than motor cortex slices after a 3 h recovery following 10 min OGD, the results were not consistent with the hypothesis, and motor cortex slices even seemed to be more vulnerable than hippocampal slices in female rats. Furthermore, within the hippocampus, the septal pole slices were expected to be more vulnerable than the temporal pole slices, which agreed with the general pattern of the current findings, however, according to the TTC assay result, after a 3 h recovery following 10 min OGD, there was no significant interaction effect between sex and region, and no significant main effect of region or sex.

Similarly, the surface expression of GluA2 was expected to decrease in all groups and in a manner that paralleled slice viability. However, according to the comparisons, although GluA2

36

surface expression decreased a bit in motor cortex, surface expression of GluA2 increased in both septal and temporal hippocampal slices, and there was no sex-region interaction and no significant main effect of region or sex.

In addition, based on the calculated effect size (partial eta-squared, η_p^2), the TTC assay showed that the strength of the interaction effect between sex and region was of a medium magnitude, the magnitude of the sex difference in metabolic function was very small, and the magnitude of the regional difference was between small and medium. In addition, the surface expression of GluA2 showed that the strength of the interaction effect between sex and region, and the magnitude of the regional difference were small to medium, and the magnitude of the sex difference was medium to large. As a result, the sex difference of GluA2 surface expression might be notable, but none of the magnitudes of difference were large ($\eta_p^2 = 0.14$ indicates a large magnitude of effect).

In summary, the alterations of metabolic function and surface expression of GluA2 were not significantly different between cortical and hippocampal slices in either male, or female rats, after a 10 min OGD challenge.

5.1 *2,3,5* - Triphenyltetrazolium chloride (TTC) assay and cell viability

According to our results, 10 min of OGD followed by 3 h of recovery lead to a 40% - 60% decrease of TTC metabolism across groups, which was considered a moderate level of injury. Furthermore, it seemed that hippocampal slices from male rats were more robust than those from female rats, and motor cortex slices were more robust in female rats. In addition, within

hippocampus, septal pole slices appeared more vulnerable than temporal pole slices from both male and female rats. However, the sex and region-based differences in viability were not statistically significant, which conflicted with the hypotheses.

One possible reason for a significant sex, or region difference not being detected via the TTC assay could be the relatively large systemic variability of the methodology, which may lead to large standard error of means (SEM). According to the hippocampal data, the trend showed that septal slices were more vulnerable than temporal slices in both male and female rats, which paralleled the assumptions, but the difference was not statistically significant. This outcome may be due to the high standard error of means (SEM) of the TTC assay data. During the TTC assay process, each group had 3 technical replicate slices and the average formazan absorbance was used to measure the concentration of the 1,3,5- triphenylformazan (TPF), which reflects the metabolism level of slices after OGD. Once control slices turned out to be not viable during the experiments, which was common and unpredictable (around 30% of the experiments), the faded slices were noticeably lighter than the others and could significantly affect the results in terms of viability. One possible solution would be to increase technical replicates in each slice group, however, this is restricted by the size of hippocampus and the slicing protocol. As a result, although TTC metabolism is one proxy for cell viability, it may not be sensitive enough to detect the existing differences, and an alternative method, such as recording field potentials, may be needed as a supplement.

In addition, the TTC assay was conducted 3 hours after OGD, and was expected to measure

the early stage of mitochondrial dysfunction. However, delayed mitochondrial dysfunction and cell death may be still on going and not completed at that time point. As a result, the possible difference may not be apparent within the first 3 h following injury. For example, HSPB8 (heat shock protein B8), which protects cells by inhibiting the mitochondrial apoptotic pathway, was overexpressed after OGD, but a statistically significant upregulation can be detected only after 4 hours of reperfusion, not after 1 hour of reperfusion (Li et al., 2018). However, it may not be feasible to simply lengthen the reperfusion time to 24 - 72 hours (as done in cell culture studies) before conducting the TTC assay. Unlike *in vitro* neuronal cell culture methods that can be kept for days to weeks, the brain slice model can only remain functionally active for several hours before further degeneration (Mielke et al., 2007), which limits the ability of the methodology to measure late cell viability differences.

5.2 Biotinylation and surface expression of GluA1 & GluA2

According to the immunoblot data, after 10 min of OGD, surface expression of GluA1 was altered across the groups. For example, both male and female rats underwent GluA1 up-regulation in septal hippocampal slices; temporal hippocampal slices, however, underwent surface GluA1 down-regulation in male rats and up-regulation in female rats, and GluA1 expression was relatively unchanged in both male and female motor cortex slices. However, there was no significant sex and region interaction, or main effect of sex, or region among the different groups.

The surface expression data of GluA2 showed neither a significant sex-region interaction,

nor a significant main effect of sex, or region. The increase of GluA2 surface expression in septal hippocampal slices seemed greater in female slices; the GluA2 surface expression in temporal hippocampal slices decreased in male rats, but increased in female rats, and the GluA2 surface expression in motor cortex slices was down-regulated more in male than in female slices. Although a two-way, mixed model ANOVA showed no significant differences, the magnitude of the sex difference was medium to large, which might be notable. To further explore the specific sex difference among different regions, a t test was applied between male and female groups, in the three individual region groups. The results showed that within temporal hippocampal slices, GluA2 surface alteration after OGD was significantly different between male and female rats. However, there was no significant difference of GluA2 surface alteration between male and female rats in septal hippocampus and motor cortex, after 10 min of OGD.

The results did not parallel the work of Blanco-Suarez and Hanley (2014). According to their neuronal culture work, after 20 min of OGD, biotinylation showed that GluA1 was relatively stably inserted at the plasma membrane in both cortical and hippocampal neurons, and GluA2 was internalized in hippocampal neurons, but not in cortical neurons. In addition, in a recent study, it was detected that the internalization of GluA2 induced by OGD was due to the endocytosis of GluA2/3, but not GluA1/2 receptors (Koszegi et al., 2017).

One possible reason for the inconsistency may be the disparity among different experimental models. Notably, the hippocampal neurons for the culture work were extracted from CA1 region (Dennis et al., 2012; Blanco-Suarez and Hanley, 2014), which is thought to be

the most vulnerable sub-region to ischemic injury within hippocampus (Dennis et al., 2012; Butler et al., 2011; Kass & Lipton, 1986), but the acute slice model utilizes slices containing all sub-regions. As a result, further study with sub-region (e.g., CA1) specific slices can be conducted to allow for a more direct comparison with the culture work; however, by removing DG and/or CA3, the reduced size of the slices may lead to a lower total protein level, which may make measuring surface expressed proteins difficult.

In addition, the slice model may still not be accurate enough to explain some multi-mechanism-affected alterations. For example, sex-specific responses to OGD could be mediated by hormone level alteration, which is, however, identical within current slice models. As the GluA2 surface expression affected by sex showed a moderate to large magnitude in this study, further experiments should be considered to better control sex-related variables to identify the underlying mechanisms. For example, the menstrual cycle of female rats can be tested to correlate with GluA2 surface expression alteration after OGD.

In this study, surface expression of GluA1 and GluA2 was detected right after 10 min OGD, without reperfusion. This design was based on the findings (Blanco-Suarez & Hanley, 2014) that surface expression alteration persists from 0 - 3 hours. However, according to our current results, the phenomenon may vary between culture and slice work. Further study could be designed to harvest slices after different lengths of reperfusion time and compare the surface expression alteration over time.

5.3 Future directions

In this study, brain slices were prepared from young adult rats. As stroke naturally has higher prevalence among older populations, some concerns about the differences between young adult brains and aging brains may be considered. In particular, both the basal level of AMPA receptors and the modifications of AMPA receptors after injury could be age-dependent (Montori et al., 2010; Wenk & Barnes, 2000). For example, according to an *in vivo* study from Montori et al. (2010), GluA1 mRNA level was higher in hippocampus, but not in cerebral cortex, and GluA2 mRNA levels was higher in both hippocampus and cerebral cortex, in the aged rats (18-month-old) than in young rats (3-month-old), at the basal level (before ischemia). After transient global ischemia, a down-regulation of GluA1 and GluA2 mRNA levels was observed in both young and aged rats, but was milder in the older group (Montori et al., 2010). The age-dependent alteration pattern of AMPA receptor subunit expression suggests that using young adult rats might not be ideal to estimate the AMPA receptor trafficking mechanism after OGD. Further experiments completed with older rats could be done to identify the possible AMPA receptor trafficking mechanisms.

6. Conclusion

According to the existing literature, ischemic stroke outcome may vary due to different factors. Although, in general, the brain is vulnerable to ischemic stroke, regional differences between hippocampus and motor cortex exist. In addition, the functionally different structures along the longitudinal axis of the hippocampus may display regional vulnerability. As well, it is also possible to observe sexual dimorphism after OGD, which may be regulated by sex hormone levels and other cellular-level factors.

Data have shown that with the current acute slice OGD model, the recoverable ischemic effect is well simulated. With the TTC assay data, regional and sex differences in mitochondrial function after OGD, are not statistically significant, which may be due to the relatively small sample size and small effect size. In addition, based on the surface expression data, a sex difference exists in GluA2 surfaces expression after OGD, and sex-region interaction exists in GluA1 surface expression after OGD. Further study that can determine synapse specific AMPA receptor alterations after OGD is needed to explore the trafficking mechanisms, and to understand the different role of hippocampus (septal *vs.* temporal) and motor cortex in the response to OGD between male and female rats.

7. Tables and Figures
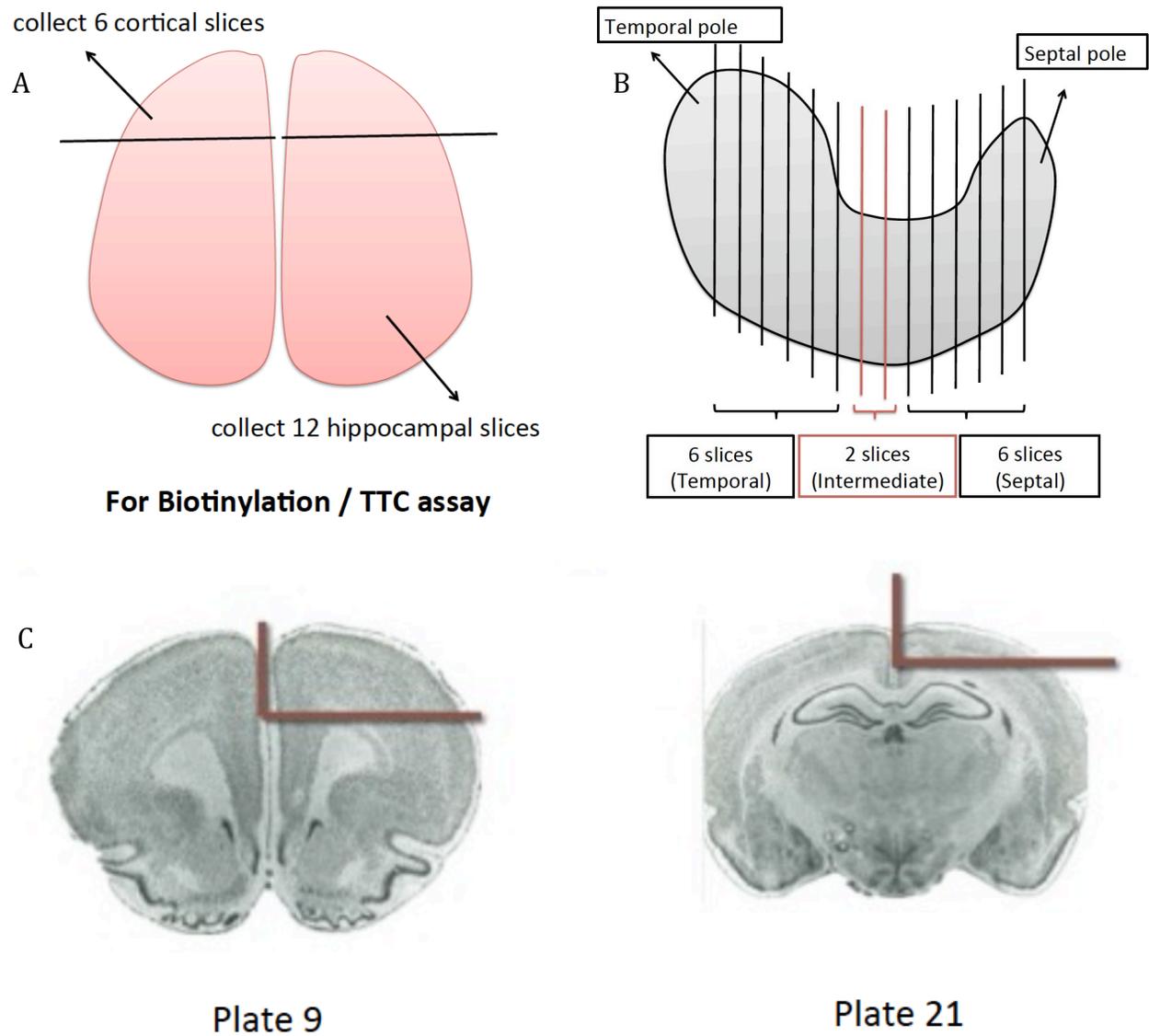
Figure 7.1 Slice preparation. A) The schematic illustrates how samples were assigned to collect hippocampal and motor cortex slices. **B)** Hippocampal slice preparation. **C)** Motor cortex slice preparation. Figure adapted from "The Rat Brain in Stereotaxic Coordinates: Compact 7th Edition" by Paxinos, G., & Watson, C., 2017, Academic Press. (57). The lines in each plate denote the region from each slice that was taken as the motor cortex.
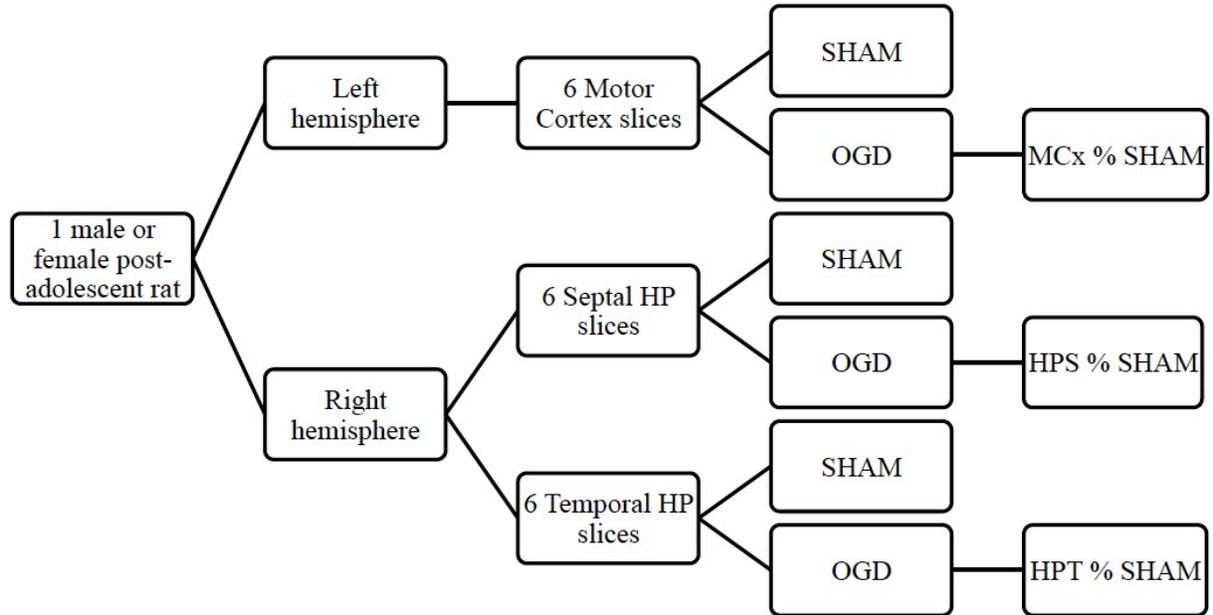
Figure 7.2 Tissue assignment across experimental groups. The schematic illustrates how tissue slices were collected and assigned to each group.
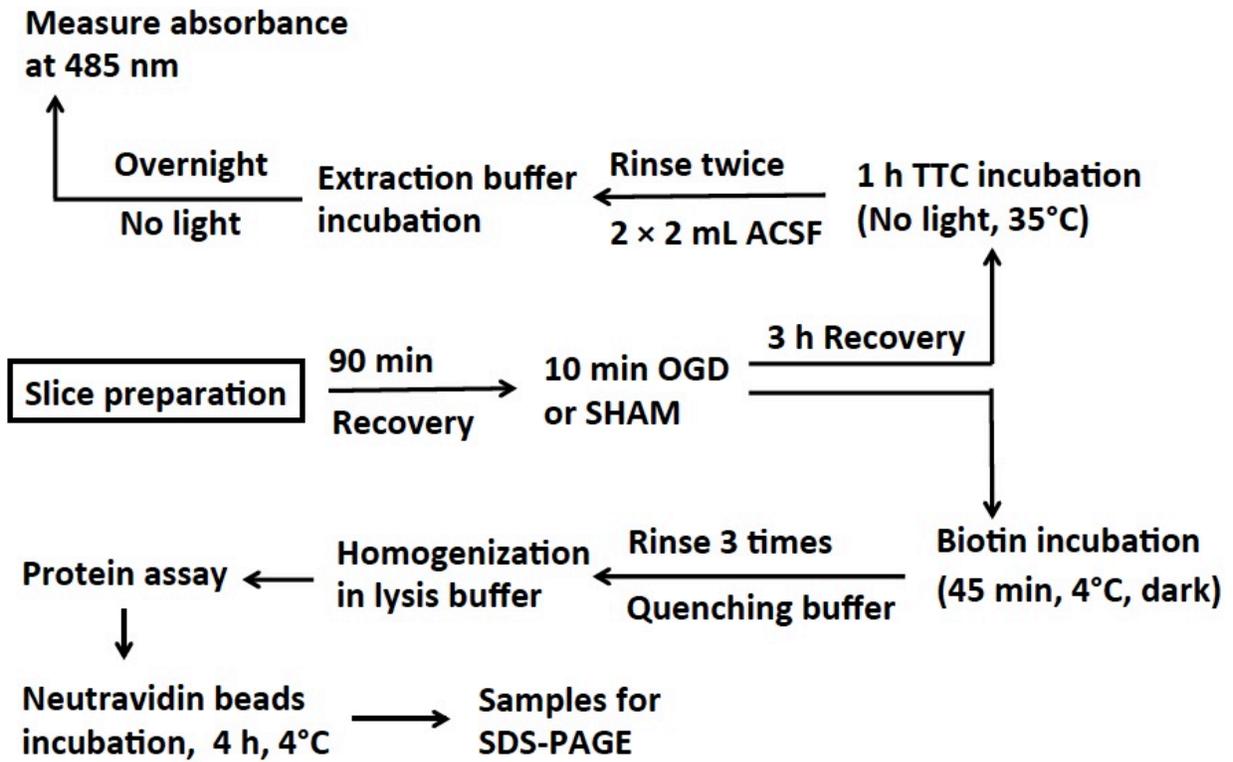
Figure 7.3 Summary of experimental protocol. The experimental process to generate the *in vitro* OGD challenge, TTC assay, and biotinylation.
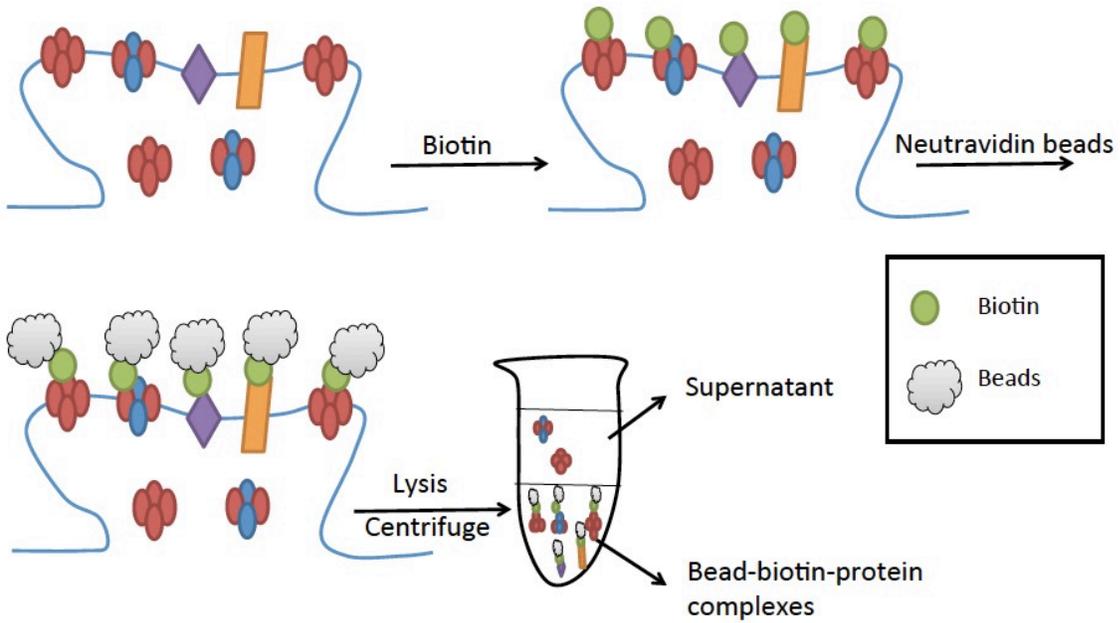
Figure 7.4 The process of biotinylation. The experimental process to generate

bead-biotin-protein complexes samples for SDS-PAGE.
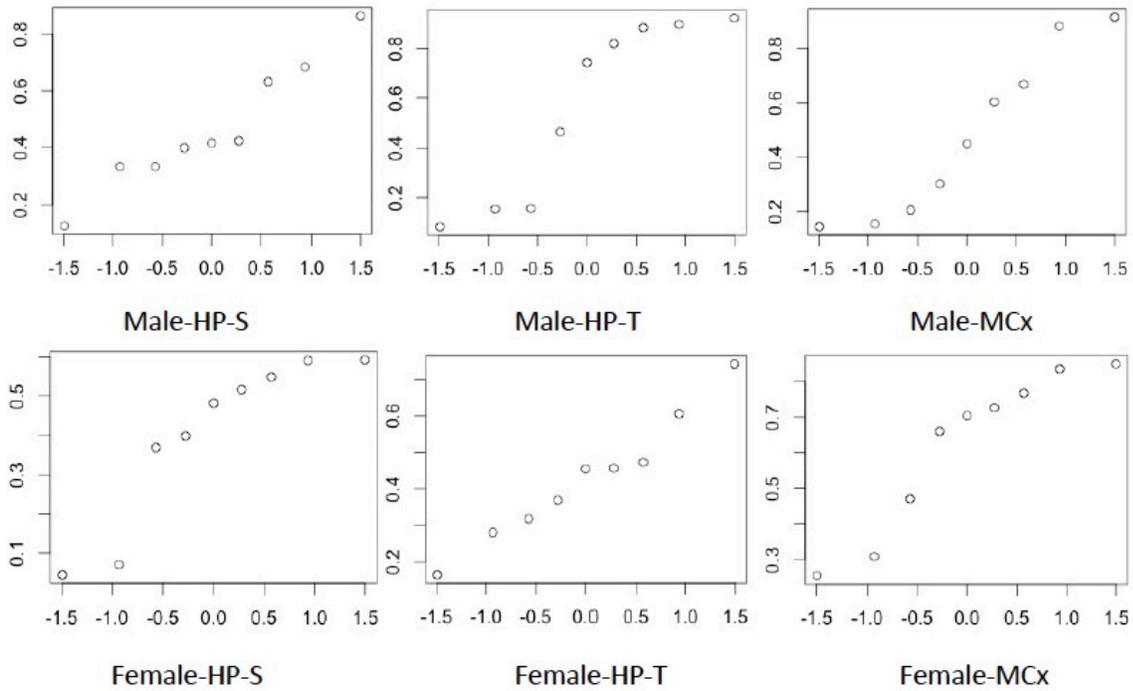
Figure 7.5 Q-Q plots of the TTC data. In this set of figures, the values of x-axis present the theoretical quantiles, and the values of y-axis present the actual sample quantiles. If the data were normally distributed, the points in the Q-Q plot would lie on a straight diagonal line.
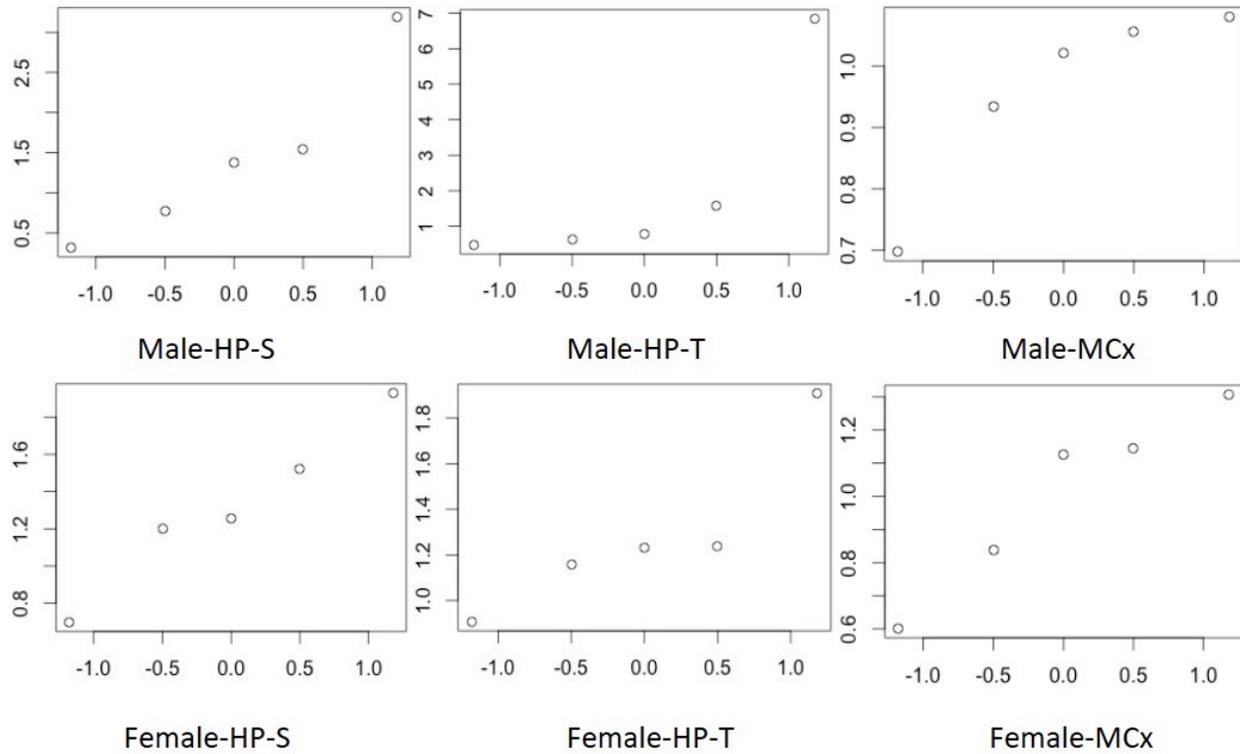
Figure 7.6 Q-Q plots of the GluA1 immunoblot results. In this set of figures, the values of x-axis present the theoretical quantiles, and the values of y-axis present the actual sample quantiles. If the data were normally distributed, the points in the Q-Q plot would lie on a straight diagonal line.
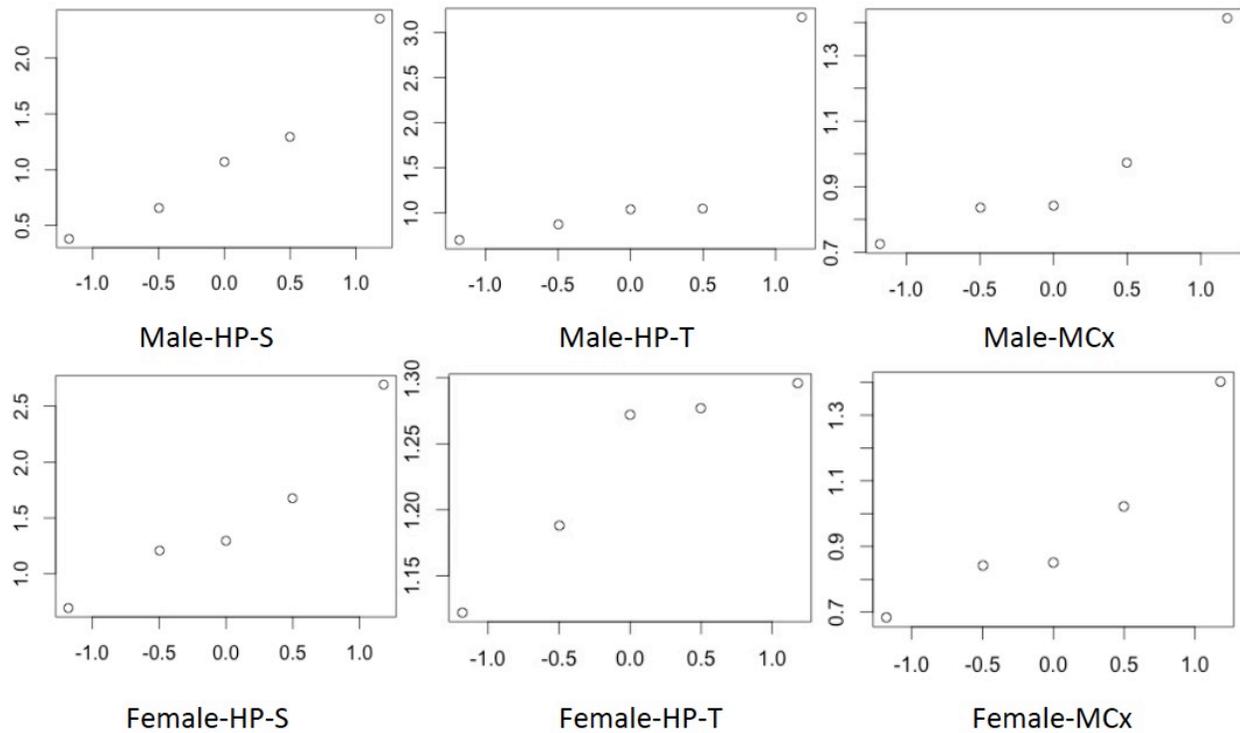
Figure 7.7 Q-Q plots of the GluA2 immunoblot results. In this set of figures, the values of

x-axis present the theoretical quantiles, and the values of y-axis present the actual sample

quantiles. If the data were normally distributed, the points in the Q-Q plot would lie on a straight

diagonal line.
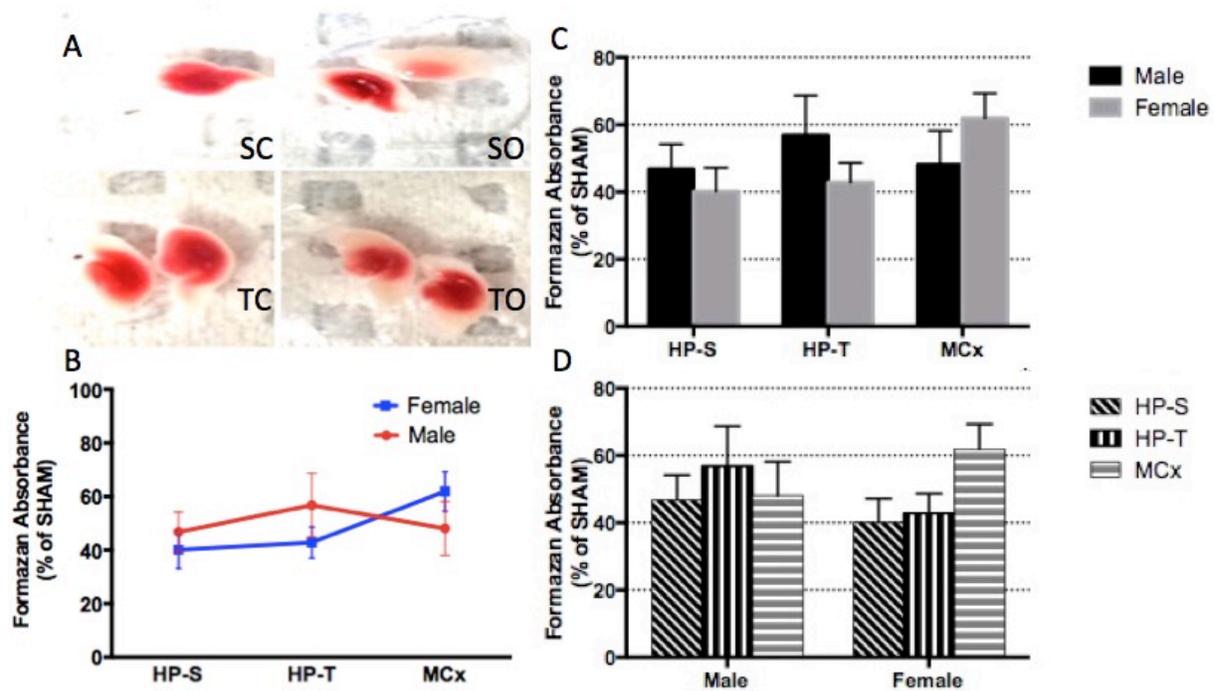
Figure 7.8 TTC assay result showed no significant sex or region difference in metabolic activity after OGD. A) Representative images of TTC assay results in one male rat. In both the septal and temporal regions, mitochondrial metabolism of TTC was significantly reduced after a 3 h recovery from 10 min of OGD. **B)** Although there appeared to be a disordinal sex-region interaction, the interaction was not statistically significant, $p = 0.84$, $F_{(2,48)} = 0.17$ **C)** The main effect of sex was compared. The male and female septal hippocampal slices underwent declines of 53.2% ± 7.38% and 59.2% ± 7.01% in metabolism; the male and female temporal hippocampal slices underwent declines of 43.2% ± 11.8% and 57.2% ± 5.79% in metabolism; the male and female motor cortex slices underwent declines of 51.9% ± 10.0% and 38.1% ± 7.38% in metabolism. $N = 9$. **D)** The main effect of region was compared. The male septal and temporal

hippocampal slices, and motor cortex slice underwent declines of 53.2% ± 7.38%, 43.2% ± 11.8%, 51.9% ± 10.0%, respectively; and the female septal and temporal hippocampal slices, and motor cortex slice underwent declines of 59.2% ± 7.01%, 57.2% ± 5.79%, 38.1% ± 7.38% 51.9% ± 10.0%, respectively. $N = 9$. Data are presented as mean ± S.E.M.
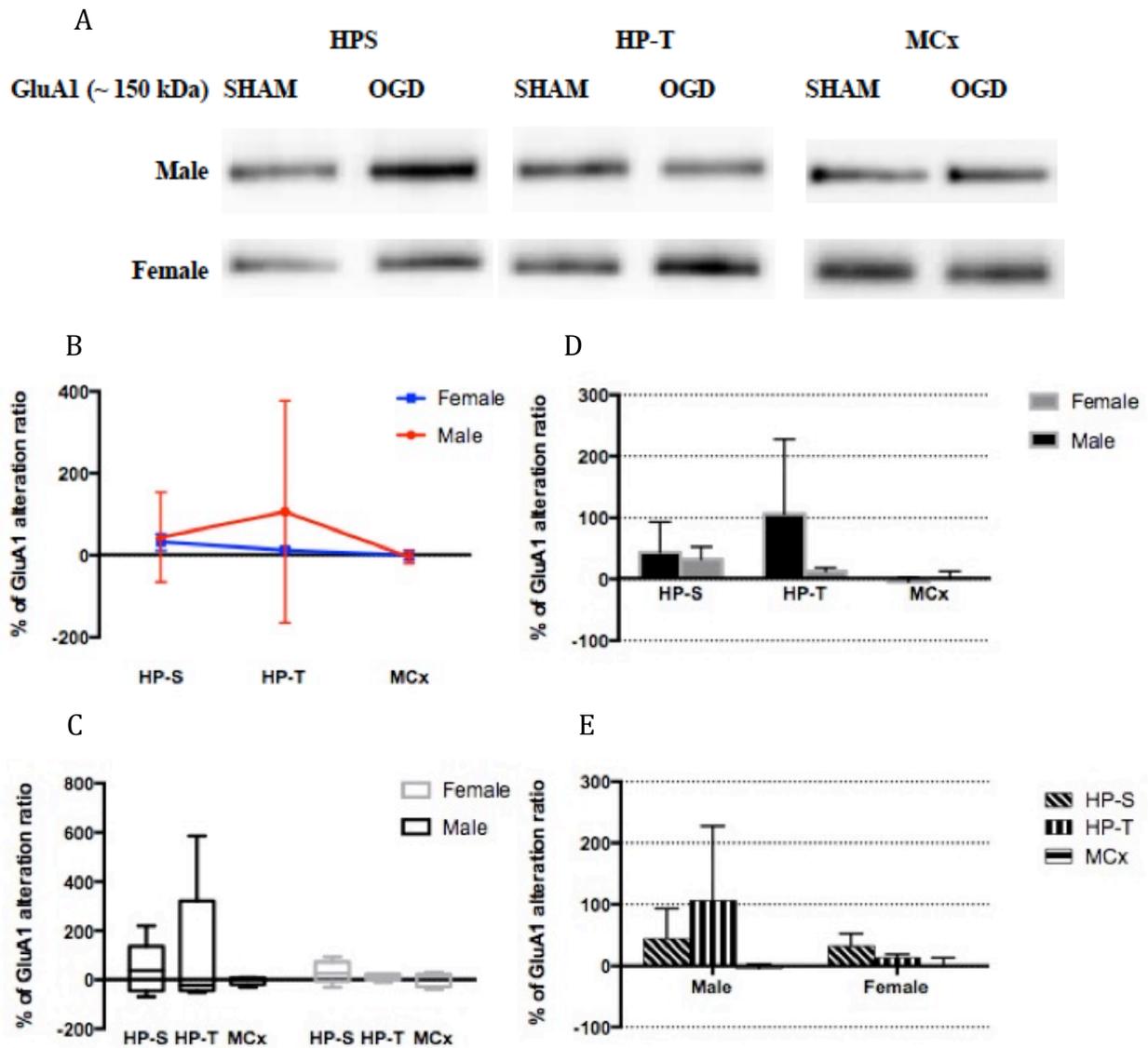
Figure 7.9 Immunoblot result showed no significant sex or region difference in GluA1 surface expression after OGD. A) Representative immunoblot images of GluA1 surface expression in one male and one female rat. **B)** There was no significant interaction effect, no significant sex, or region difference in GluA1 surface expression, based on the two-way, mixed ANOVA results. GluA1 surface expression alteration ratios (presented as a percent of SHAM) increased 43.9% ± 48.94% in septal hippocampal slices, and decreased 13.52% ± 19.01%, and

4.22% ± 6.95% in temporal hippocampal slices, and motor cortex slices, respectively, after OGD

in male rats. $N = 5$. GluA1 surface expression alteration ratios (presented as a percent of SHAM)

increased 32.1% ± 20.2%, 20.9 % ± 1.41%, and 0.34% ± 12.58 % in septal hippocampal slices,

temporal hippocampal slices, and motor cortex slices, respectively, after OGD in female rats. $N =$

5. **C)** The box plot for GluA1 surface expression. **D)** The main effect of sex was compared. **E)**

The main effect of region was compared. % of GluA1 alteration ratio

$= \frac{GluA1\ expression\ of\ OGD\ group}{GluA1\ expression\ of\ SHAM} \times 100\% - 100\%$. Data are presented as mean ± S.E.M.
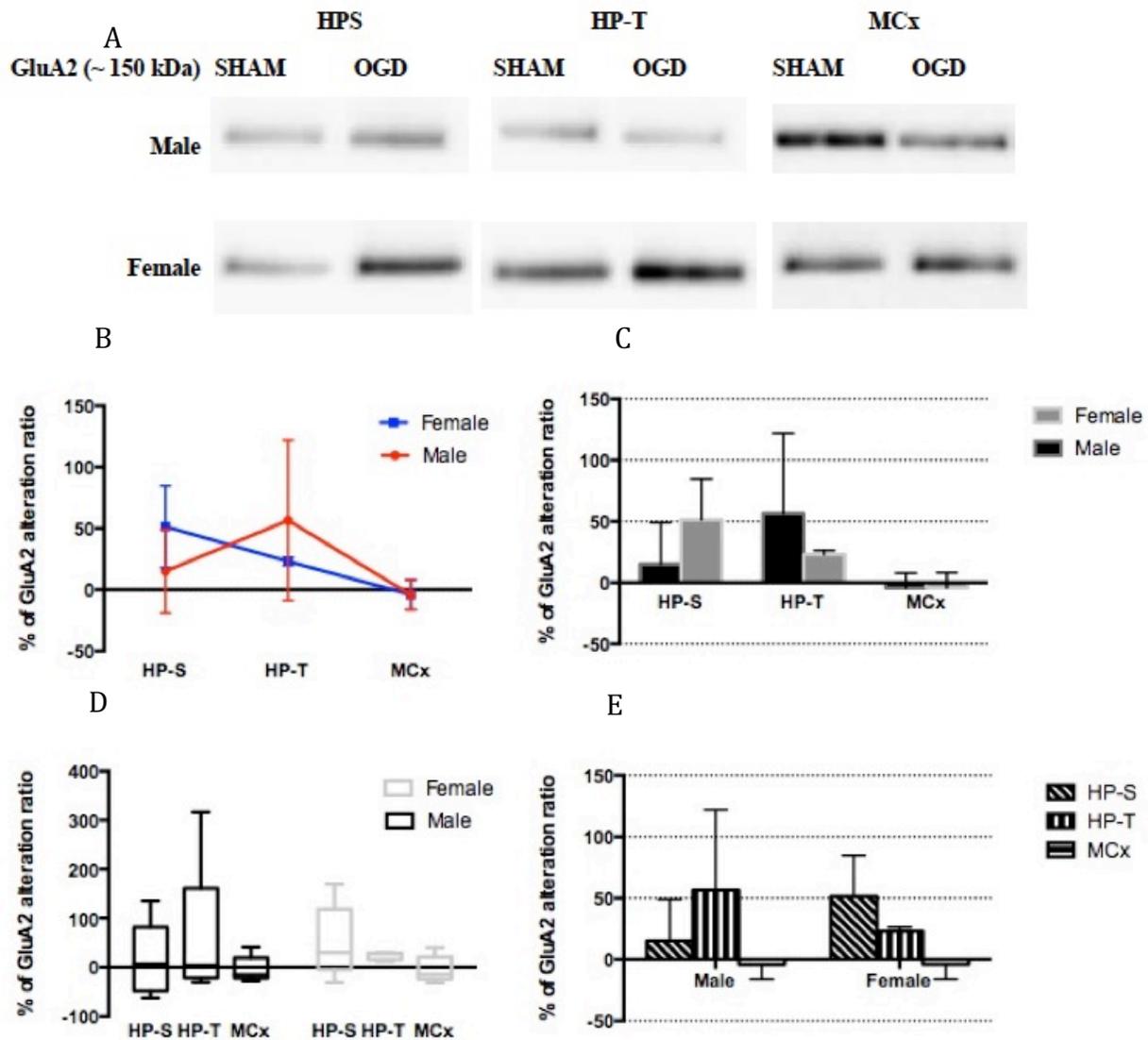
Figure 7.10 Immunoblot result showed no significant sex or region difference in GluA2 surface expression after OGD. A) Representative immunoblot images of GluA2 surface expression in one male and one female rat. **B)** There was no significant interaction effect, no significant sex, or region difference in GluA2 surface expression, based on the two-way, mixed ANOVA results. GluA2 surface expression alteration ratios (presented as a percent of SHAM) increased 15.1 % ± 34.0 % in septal hippocampal slices, and decreased 8.47 % ± 6.38 %, and

15.6% ± 3.93% in temporal hippocampal slices, and motor cortex slices, respectively, after OGD

in male rats. N = 5. GluA1 surface expression alteration ratios (presented as a percent of SHAM)

of female rats (presented as a percent of SHAM) increased 51.3 % ± 33.4 %, and 23.1 % ± 3.30%

in septal hippocampal slices, and temporal hippocampal slices, and decreased 4.00% ± 12.3% in

Motor cortex slices, after 10 min OGD. N = 5. **C)** The box plot for GluA2 surface expression. **D)**

The main effect of sex was compared. **E)** The main effect of region was compared. % of GluA2

alteration ratio $= \frac{GluA2\ expression\ of\ OGD\ group}{GluA2\ expression\ of\ SHAM} \times 100\% - 100\%$. Data are presented as mean ±

S.E.M.

		Male			Female		
		HP-S	HP-T	MCx	HP-S	HP-T	MCx
Q_1		0.333	0.156	0.207	0.368	0.317	0.471
Q_3		0.632	0.883	0.669	0.549	0.472	0.767
IQR		0.299	0.727	0.462	0.181	0.155	0.296
Outlier fence	Min value (Q_1 - 3 IQR)	-0.564	-2.025	-1.179	-0.175	-0.148	-0.417
	Max value (Q_3 + 3 IQR)	1.529	3.064	2.055	1.092	0.937	1.655
No. of Outlier(s)		**0**	**0**	**0**	**0**	**0**	**0**

Table 7.1 TTC assay outlier test results. Q_1, lower quartiles; Q_3, upper quartiles; IQR, inter quartile range; HP-S, septal hippocampus; HP-T, temporal hippocampus; MCx, motor cortex.

		Male	Female
N		9	9
Fligner-Killeen test (*p* value)		0.209	
HP-S	**Mean % SHAM**	46.8%	40.1%
	SEM	7.38%	7.01%
	Shapiro-Wilk test (*p* value)	0.653	0.0367 *
	Skewness	0.500	-1.093
	Kurtosis	0.0714	-0.205
HP-T	**Mean % SHAM**	56.8%	42.8%
	SEM	11.9%	5.79%
	Shapiro-Wilk test (*p* value)	0.0363 *	0.938
	Skewness	-0.453	0.392
	Kurtosis	-1.959	0.202
MCx	**Mean % SHAM**	48.1%	61.9%
	SEM	10.0%	7.38%
	Shapiro-Wilk test (*p* value)	0.259	0.133
	Skewness	0.329	-0.807
	Kurtosis	-1.533	-0.891

Table 7.2 Assessment of homogeneity of variance and distribution characteristics for the TTC data. Data presented as % of SHAM TTC formazan absorbance. Standard error of the mean (SEM) was calculated for each group. Homogeneity of variances across the groups was determined by the Fligner-Killeen test, and the assumption of homogeneity of variance could not be rejected. Normality of distributions for the groups was examined by the Shapiro-Wilk test, and the assumption of normality might not be accepted in the female septal hippocampus group and the male temporal hippocampus group, *, p value < 0.05. Skewness and kurtosis were also calculated to evaluate normality. Skewness less than -1, or greater than 1 indicates a highly skewed distribution, while kurtosis close to 0 indicates a normal distribution.

	F value	df	Sum of squares	Mean Square	p value	η_p^2
Sex	0.244	1	0.0159	0.0159	0.624	0.00223
Region	1.113	2	0.145	0.0726	0.337	0.0373
Sex: Region	0.172	2	0.0224	0.0112	0.843	0.0565
Residuals	NA	45	2.935	0.0652	NA	NA

Table 7.3 Summary of two-way, mixed model ANOVA results for the TTC assay data.

There was no significant sex-region interaction in metabolic activity after OGD. As well, there were no significant sex, or region-based differences in metabolic activity after OGD. Interpretation of effect sizes measured by η_p^2 is as follows: Small, $\eta_p^2 = 0.01$, medium, $\eta_p^2 = 0.06$, large, $\eta_p^2 = 0.14$. df, degree of freedom.

GluA1		Male			Female		
		HP-S	HP-T	MCx	HP-S	HP-T	MCx
Q_1		0.772	0.629	0.934	1.158	0.838	1.208
Q_3		1.541	1.576	1.056	1.238	1.145	1.676
IQR		0.769	0.948	0.122	0.080	0.306	0.468
Outlier fence	Min value (Q_1 - 3 IQR)	-1.536	-2.214	0.569	0.236	0.918	-0.081
	Max value (Q_3 + 3 IQR)	3.850	4.419	1.421	2.487	1.478	2.065
Rat No. of Outlier(s)		0	1	0	0	2	0

Table 7.4 Outlier results for the immunoblot data of GluA1 surface expression. The outliers were identified by Tukey's methods. The fence used to identify outliers was ($Q_1 - 3$ IQR, $Q_3 + 3$ IQR). Temporal hippocampal data from rat male 4, female 1, and female 2 were classified as outliers. Q_1, lower quartiles; Q_3, upper quartiles; IQR, inter quartile range; HP-S, septal hippocampus; HP-T, temporal hippocampus; MCx, motor cortex.

		Male	Female
N		5	5
Fligner-Killeen test (*p* value)		0.679	
HP-S	**Mean % SHAM**	144%	132%
	SEM	48.9%	20.2%
	Shapiro-Wilk test (*p* value)	0.515	0.945
	Skewness	1.163	-0.0491
	Kurtosis	1.767	0.668
HP-T	**Mean % SHAM**	206%	129%
	SEM	121.2%	16.6%
	Shapiro-Wilk test (*p* value)	0.006 *	0.190
	Skewness	2.105	1.462
	Kurtosis	4.486	3.076
MCx	**Mean % SHAM**	95.8%	100%
	SEM	6.95%	12.6%
	Shapiro-Wilk test (*p* value)	0.141	0.6144
	Skewness	-1.615	-0.694
	Kurtosis	2.482	-0.792

Table 7.5 Assessment of homogeneity of variance and distribution characteristics for the immunoblot data of GluA1 surface expression Data presented as % of SHAM. Standard error of the mean (SEM) was calculated for each group. Homogeneity of variances for GluA1 surface expression was test by the Fligner-Killeen test, and the assumption of homogeneity of variances could not be rejected. Normality of distribution for GluA1 surface expression was test by the Shapiro-Wilk test, and the assumption of normality could not be rejected, except in the male temporal hippocampus group, *, p value < 0.05. Skewness and kurtosis were also calculated to evaluate normality. Skewness less than -1, or greater than 1 indicates a highly skewed distribution, while kurtosis close to 0 indicates a normal distribution.

	F value	df	Sum of squares	Mean Square	p value	η_p^2
Sex	1.709	1	3.55	3.547	0.205	0.048
Region	0.096	2	0.40	0.198	0.909	0.011
Sex: Region	0.934	2	3.88	1.939	0.409	0.015
Residuals	NA	21	43.58	2.075	NA	NA

Table 7.6 Summary of two-way, mixed model ANOVA results for the immunoblot results of GluA1 surface expression. There was no significant sex-region interaction in metabolic activity after OGD. As well, there were no significant sex, or region-based differences in metabolic activity after OGD. Interpretation of effect sizes measured by η_p^2 is as follows: Small, $\eta_p^2 = 0.01$, medium, $\eta_p^2 = 0.06$, large, $\eta_p^2 = 0.14$. df, degree of freedom.

GluA2		Male			Female		
		HP-S	HP-T	MCx	HP-S	HP-T	MCx
Q_1		0.656	0.873	0.836	1.208	1.188	0.842
Q_3		1.294	1.048	0.973	1.676	1.277	1.022
IQR		0.638	0.175	0.137	0.468	0.089	0.180
Outlier fence	Min value (Q_1 - 3 IQR)	-1.258	0.350	0.425	-0.196	0.920	0.302
	Max value (Q_3 + 3 IQR)	3.207	1.571	1.383	3.081	1.545	1.561
Rat No. of Outlier(s)		0	1	1	0	0	0

Table 7.7 Outlier results for the immunoblot data of GluA2 surface expression. The outliers were identified by Tukey's methods. The outlier fence used to identify outliers was ($Q_1 - 3$ IQR, $Q_3 + 3$ IQR). Temporal hippocampus and motor cortex data from rat male 4 were classified as outliers. Q_1, lower quartiles; Q_3, upper quartiles; IQR, inter quartile range; HP-S, septal hippocampus; HP-T, temporal hippocampus; MCx, motor cortex.

		Male	Female
N		5	5
Fligner-Killeen test (*p* value)		0.523	
HP-S	**Mean % SHAM**	115%	151%
	SEM	34.0%	33.4%
	Shapiro-Wilk test (*p* value)	0.590	0.610
	Skewness	1.101	1.057
	Kurtosis	1.372	1.645
HP-T	**Mean % SHAM**	136%	123%
	SEM	45.5%	3.30%
	Shapiro-Wilk test (*p* value)	0.006*	0.245
	Skewness	2.125	-0.972
	Kurtosis	4.625	-0.833
MCx	**Mean % SHAM**	95.8%	96.0%
	SEM	12.1%	12.3%
	Shapiro-Wilk test (*p* value)	0.137	0.410
	Skewness	1.675	1.263
	Kurtosis	3.022	1.766

Table 7.8 Assessment of homogeneity of variance and distribution characteristics for the immunoblot data of GluA2 surface expression Data presented as % of SHAM. Standard error of the mean (SEM) was calculated for each group. Homogeneity of variances for GluA2 surface expression was test by the Fligner-Killeen test, and the assumption of homogeneity of variances could not be rejected. Normality of distribution for GluA2 surface expression was test by the Shapiro-Wilk test, and the assumption of normality could not be rejected except in the male temporal hippocampus group, *, *p* value < 0.05. Skewness and kurtosis were also calculated to evaluate normality. Skewness less than -1, or greater than 1 indicates a highly skewed distribution, while kurtosis close to 0 indicates a normal distribution.

	F value	df	Sum of squares	Mean Square	p value	η_p^2
Sex	2.325	1	3.499	3.499	0.142	0.042
Region	0.020	2	0.061	0.030	0.980	0.010
Sex: Region	2.398	2	7.218	3.609	0.115	0.055
Residuals	NA	21	31.605	1.505	NA	NA

Table 7.9 Summary of two-way, mixed model ANOVA results for the immunoblot results of GluA2 surface expression. There was no significant sex-region interaction in metabolic activity after OGD. As well, there were no significant sex, or region-based differences in metabolic activity after OGD. Interpretation of effect sizes measured by η_p^2 is as follows: Small, $\eta_p^2 = 0.01$, medium, $\eta_p^2 = 0.06$, large, $\eta_p^2 = 0.14$. df, degree of freedom.

p value (adjusted)	GluA1	GluA2
female,hps - male,hps	0.999	0.996
female,hps - female,hpt	0.999	0.999
female,hps - male,hpt	0.959	0.966
female,hps - female,mcx	0.992	0.955
female,hps - male,mcx	0.943	0.946
male,hps - female,hpt	0.998	0.999
male,hps - male,hpt	0.907	0.999
male,hps - female,mcx	0.966	0.766
male,hps - male,mcx	0.983	0.998
female,hpt - male,hpt	0.987	0.998
female,hpt - female,mcx	0.999	0.821
female,hpt - male,mcx	0.879	0.995
male,hpt - female,mcx	0.999	0.581
male,hpt - male,mcx	0.562	0.999
female,mcx - male,mcx	0.709	0.523

Table 7.10 Post-hoc test (Tukey's test) for immunoblot analysis. There is no significant

between-group difference of GluA1 and/or GluA2 surface expression after OGD, *, Tukey's test,

$p < 0.05$.

8. References

1. Ahlbom, E., Prins, G. S., & Ceccatelli, S. (2001). Testosterone protects cerebellar granule cells from oxidative stress-induced cell death through a receptor mediated mechanism. *Brain research*, 892(2), 255-262.

2. American Heart Association. (2017). Ischemic Strokes (Clots). [online] Available at: http://www.strokeassociation.org/STROKEORG/AboutStroke/TypesofStroke/IschemicClots/Ischemic-Strokes-Clots_UCM_310939_Article.jsp#.WbelldOGNmB [Accessed 02 Sep. 2017].

3. Armitage, J., Baigent, C., Barnes, E., Betteridge, D. J., Blackwell,... & Clearfield, M. (2019). Efficacy and safety of statin therapy in older people: a meta-analysis of individual participant data from 28 randomised controlled trials. *The Lancet*, 393(10170), 407-415.

4. Ashton, D., Van Reempts, J., Haseldonckx, M., & Willems, R. (1989). Dorsal-ventral gradient in vulnerability of CA1 hippocampus to ischemia: a combined histological and electrophysiological study. *Brain research*, 487(2), 368-372.

5. Atlantis, T. (2004). Association of outcome with early stroke treatment: pooled analysis of ATLANTIS, ECASS, and NINDS rt-PA stroke trials. *The Lancet*, 363(9411), 768-774.

6. Au, K. N., & Gurd, J. W. (1995). Tyrosine phosphorylation in a model of ischemia using the rat hippocampal slice: specific, long-term decrease in the Tyrosine phosphorylation of the postsynaptic glycoprotein PSD-GP180. *Journal of Neurochemistry*, 65(4), 1834-1841.

7. Bakker, M., & Wicherts, J. M. (2014). Outlier removal and the relation with reporting errors and quality of psychological research. *PLoS One*, 9(7), e103360.

8. Bannerman, D. M., Rawlins, J. N. P., McHugh, S. B., Deacon, R. M. J., Yee, B. K., Bast, T., Zhang, W.-N, Pothuizen, J. H.H, & Feldon, J (2004). Regional dissociations within the hippocampus—memory and anxiety. *Neuroscience & Biobehavioral Reviews*, 28(3), 273-283.

9. Beattie, E. C., Carroll, R. C., Yu, X., Morishita, W., Yasuda, H., von Zastrow, M., & Malenka, R. C. (2000). Regulation of AMPA receptor endocytosis by a signaling mechanism shared with LTD. *Nature Neuroscience*, 3(12), 1291.

10. Bedford, F. K. (2009). Receptor Trafficking. *In Encyclopedia of Neuroscience* (pp. 3385-3389). Springer Berlin Heidelberg.

11. Bekiari Ch., Grivas I., Giannakopoulou A., Michaloudi-Pavou H., Kostopoulos G., & Papadopoulos G.C. (2015). Dentate gyrus variation along its septo-temporal axis: structure and function in health and disease. *In: Dentate Gyrus*. pp 138-197. Greece: Nova Science Publishers Inc.

12. Blanco-Suarez, E., & Hanley, J. G. (2014). Distinct subunit-specific α-Amino-3-hydroxy-5-methyl-4-isoxazolepropionic Acid (AMPA) receptor trafficking mechanisms in cultured cortical and hippocampal neurons in response to oxygen and glucose deprivation. *Journal of Biological Chemistry*, 289(8), 4644-4651.

13. Bonfoco, E., Krainc, D., Ankarcrona, M., Nicotera, P., & Lipton, S. A. (1995). Apoptosis and necrosis: two distinct events induced, respectively, by mild and intense insults with

N-methyl-D-aspartate or nitric oxide/superoxide in cortical cell cultures. *Proceedings of the National Academy of Sciences*, 92(16), 7162-7166.

14. Broughton, B. R., Reutens, D. C., & Sobey, C. G. (2009). Apoptotic mechanisms after cerebral ischemia. *Stroke,* 40(5), e331-e339.

15. Busl, K. M., & Greer, D. M. (2010). Hypoxic-ischemic brain injury: pathophysiology, neuropathology and mechanisms. *NeuroRehabilitation*, *26*(1), 5-13.

16. Cai, M., Ma, Y. L., Qin, P., Li, Y., Zhang, L. X., Nie, H., Peng, Z., Dong, H., Dong, H. L., Hou, W. G., & Xiong, L. Z. (2014). The loss of estrogen efficacy against cerebral ischemia in aged postmenopausal female mice. *Neuroscience Letters,* 558, 115-119.

17. Carvalho, A. L., Duarte, C. B., & Carvalho, A. P. (2000). Regulation of AMPA receptors by phosphorylation. *Neurochemical research*, 25(9-10), 1245-1255.

18. Cervos-Navarro, J., & Diemer, N. H. (1991). Selective vulnerability in brain hypoxia. *Critical reviews in neurobiology*, 6(3), 149-182.

19. Chen, H. M., Wang, W. T., Chiang, C. E., Sung, S. S., You, L. K., Chuang, S. Y. (2015). Effects of antihypertensive therapies on primary and secondary prevention of stroke: Systematic review and network meta-analysis. In *European Heart Journal*, 36, 849-1187 34.

20. Cheng, J., Alkayed, N. J., & Hurn, P. D. (2007). Deleterious effects of dihydrotestosterone on cerebral ischemic injury. *Journal of Cerebral Blood Flow & Metabolism*, 27(9), 1553-1562.

21. Cheng J., Hurn P.D. (2010). Sex shapes experimental ischemic brain injury. *Steroids*. 75: 754-759.

22. Cherubini, A., Ruggiero, C., Polidori, M. C., & Mecocci, P. (2005). Potential markers of oxidative stress in stroke. *Free Radical Biology and Medicine*, 39(7), 841-852. 39.

23. Conover, W. J., Johnson, M. E., & Johnson, M. M. (1981). A comparative study of tests for homogeneity of variances, with applications to the outer continental shelf bidding data. *Technometrics*, 23(4), 351-361.

24. Cousineau, D., & Chartier, S. (2010). Outliers detection and treatment: a review. *International Journal of Psychological Research*, 3(1), 58-67.

25. Czerniawski J., Yoon T., Otto T. (2009). Dissociating space and trace in dorsal and ventral hippocampus. *Hippocampus*. 19: 20-32.

26. Czerniczyniec, A., La Padula, P., Bustamante, J., Karadayian, A. G., Lores-Arnaiz, S., & Costa, L. E. (2015). Mitochondrial function in rat cerebral cortex and hippocampus after short-and long-term hypobaric hypoxia. *Brain research*, 1598, 66-75.

27. D'agostino, R. B., Belanger, A., & D'Agostino Jr, R. B. (1990). A suggestion for using powerful and informative tests of normality. *The American Statistician*, 44(4), 316-321.

28. De Butte-Smith, M., Gulinello, M., Zukin, R. S., & Etgen, A. M. (2009). Chronic estradiol treatment increases CA1 cell survival but does not improve visual or spatial recognition memory after global ischemia in middle-aged female rats. *Hormones and Behavior*, 55(3), 442-453.

29. de Lores Arnaiz, G. R., & Ordieres, M. G. L. (2014). Brain Na$^+$, K$^+$-ATPase activity in aging

and disease. *International Journal of Biomedical Science*: IJBS, 10(2), 85.

30. Dennis, S. H., Jaafari, N., Cimarosti, H., Hanley, J. G., Henley, J. M., & Mellor, J. R. (2011). Oxygen/glucose deprivation induces a reduction in synaptic AMPA receptors on hippocampal CA3 neurons mediated by mGluR1 and adenosine A3 receptors. *Journal of Neuroscience*, 31(33), 11941-11952.

31. Derkach, V. A., Oh, M. C., Guire, E. S., & Soderling, T. R. (2007). Regulatory mechanisms of AMPA receptors in synaptic plasticity. *Nature Reviews Neuroscience*, 8(2), 101-113.

32. Diniz, C. R., Casarotto, P. C., & Joca, S. R. (2016). NMDA-NO signaling in the dorsal and ventral hippocampus time-dependently modulates the behavioral responses to forced swimming stress. *Behavioural brain research*, 307, 126-136.

33. Dirnagl, U., Iadecola, C., & Moskowitz, M. A. (1999). Pathobiology of ischaemic stroke: an integrated view. *Trends in Neurosciences*, 22(9), 391-397.

34. Donna, GA, Fisher, M., Macleod M., & Davis SM. (2008). Stroke. *Lancet*, 370, 1-12.

35. Dougherty, K. A., Islam, T., & Johnston, D. (2012). Intrinsic excitability of CA1 pyramidal neurones from the rat dorsal and ventral hippocampus. *The Journal of Physiology*, 590(22), 5707-5722. 53.

36. Du, L., Bayir, H., Lai, Y., Zhang, X., Kochanek, P. M., Watkins, S. C., Graham, S. H. & Clark, R. S. (2004). Innate gender-based proclivity in response to cytotoxicity and programmed cell death pathway. *Journal of Biological Chemistry*, 279(37), 38563-38570.

37. Fanaei, H., Karimian, S. M., Sadeghipour, H. R., Hassanzade, G., Kasaeian, A., Attari, F., Attarid, F., Khayatg, S., Ramezanih, V. & Javadimehr, M. (2014). Testosterone enhances functional recovery after stroke through promotion of antioxidant defenses, BDNF levels and neurogenesis in male rats. *Brain research*, 1558, 74-83.

38. Fanselow M.S., Dong H.W. (2010). Are the dorsal and ventral hippocampus functionally distinct structures? *Neuron*. 65(1): 1-25.

39. Farber, J. L. (1990). The role of calcium ions in toxic cell injury. *Environmental health perspectives*, 84, 107-111.

40. Feigin, V. L., Roth, G. A., Naghavi, M., Parmar, P., Krishnamurthi, R., Chugh, S., Mensah,G.A., Norrving, B., Shiue, I., Ng, M., & Estep, K. (2016). Global burden of stroke and risk factors in 188 countries, during 1990–2013: a systematic analysis for the Global Burden of Disease Study 2013. *The Lancet Neurology*, *15*(9), 913-924.

41. Floriou-Servou, A., von Ziegler, L., Stalder, L., Sturman, O., Privitera, M., Rassi, A., Cremonesic, A., Thönyd, B. & Bohacek, J. (2018). Distinct proteomic, transcriptomic, and epigenetic stress responses in dorsal and ventral hippocampus. *Biological psychiatry*, 84(7), 531-541.

42. Förstermann, U., & Sessa, W. C. (2011). Nitric oxide synthases: regulation and function. *European Heart Journal*, 33(7), 829-837.

43. Fu, X. Z., Zhang, Q. G., Meng, F. J., & Zhang, G. Y. (2004). NMDA receptor-mediated immediate Ser831 phosphorylation of GluR1 through CaMKIIα in rat hippocampus during early global ischemia. *Neuroscience Research,* 48(1), 85-91.

44. Ghasemi, A., & Zahediasl, S. (2012). Normality tests for statistical analysis: a guide for non-statisticians. *International journal of endocrinology and metabolism*, 10(2), 486.

45. Gibson, C. L. (2013). Cerebral ischemic stroke: is gender important?. *Journal of Cerebral Blood Flow & Metabolism*, 33(9), 1355-1361.

46. Godwin, K. M., Wasserman, J., & Ostwald, S. K. (2011). Cost associated with stroke: outpatient rehabilitative services and medication. *Topics in Stroke Rehabilitation*, *18*(sup1), 676-684.

47. Goyal, R. K., & Chaudhury, A. (2013). Structure activity relationship of synaptic and junctional neurotransmission. *Autonomic Neuroscience*, 176(1), 11-31.

48. Gulyaeva, N. V. (2018). Functional neurochemistry of the ventral and dorsal hippocampus: stress, depression, dementia and remote hippocampal damage. *Neurochemical Research*, 1-17.

49. Hackam, D. G., & Spence, J. D. (2007). Combining multiple approaches for the secondary prevention of vascular events after stroke. *Stroke*, 38(6), 1881-1885.

50. Hacke, W., Kaste, M., Bluhmki, E., Brozman, M., Dávalos, A., Guidetti, D., Larrue, V., Lees, K.R., Medeghri, Z., Machnig, T., Schneider, D., Kummer, R., Wahlgren, N., & Toni, D. (2008). Thrombolysis with alteplase 3 to 4.5 hours after acute ischemic stroke. *New England Journal of Medicine*, 359(13), 1317-1329.

51. Hakim, A. M. (1998). Ischemic penumbra The therapeutic window. *Neurology*, 51(3 Suppl 3), S44-S46.

52. Hanley, J. G. (2014). Subunit-specific trafficking mechanisms regulating the synaptic expression of Ca 2^{+}-permeable AMPA receptors. *Seminars in Cell & Developmental Biology,* 27, 14-22). Academic Press.

53. Hart, S. A., Patton, J. D., & Woolley, C. S. (2001). Quantitative analysis of ERα and GAD colocalization in the hippocampus of the adult female rat. *Journal of Comparative Neurology*, 440(2), 144-155.

54. Hawk, T., Zhang, Y. Q., Rajakumar, G., Day, A. L., & Simpkins, J. W. (1998). Testosterone increases and estradiol decreases middle cerebral artery occlusion lesion size in male rats. *Brain research*, 796(1-2), 296-298.

55. Hayashi, Y., Shi, S. H., Esteban, J. A., Piccini, A., Poncer, J. C., & Malinow, R. (2000). Driving AMPA receptors into synapses by LTP and CaMKII: requirement for GluR1 and PDZ domain interaction. *Science*, 287(5461), 2262-2267.

56. Hebert, D., Lindsay, M. P., McIntyre, A., Kirton, A., Rumney, P. G., Bagg, S., Bayley, M., Dowlatshahi, D., Dukelow, S., Garnhum, M., Glasser, E., Halabi, M., Kang, E., MacKay-Lyons, M., Martino, R., Rochette, A., Rowe, S., Salbach, N., Semenko, B., Stack, B., Swinton, L., Weber, V., Mayer, M., Verrilli, S., DeVeber, G., Andersen, J., Barlow, K., Cassidy, C., Dilenge, M., Fehlings, D., Hung, Y., Iruthayarajah, J., Lenz, L., Majnemer, A., Purtzki, J., Rafay, M.,

Sonnenberg, L. K., Townley, A., Janzen, S., Foley, N. & Teasell, R. (2016). Canadian stroke best practice recommendations: stroke rehabilitation practice guidelines, update 2015. *International Journal of Stroke*, 11(4), 459-484.

57. Henke, P. G. (1990). Hippocampal pathway to the amygdala and stress ulcer development. *Brain research bulletin*, 25(5), 691-695.

58. Henley, J. M., & Wilkinson, K. A. (2016). Synaptic AMPA receptor composition in development, plasticity and disease. *Nature Reviews Neuroscience*, 17(6), 337-351.

59. Hollmann, M., Maron, C., & Heinemann, S. (1994). N-glycosylation site tagging suggests a three transmembrane domain topology for the glutamate receptor GluR1. *Neuron, 13(6)*, 1331-1343.

60. Isaeva, E., Romanov, A., Holmes, G. L., & Isaev, D. (2015). Status epilepticus results in region-specific alterations in seizure susceptibility along the hippocampal longitudinal axis. *Epilepsy Research*, 110, 166-170.

61. Jaafari, N., Henley, J. M., & Hanley, J. G. (2012). PICK1 mediates transient synaptic expression of GluA2-lacking AMPA receptors during glycine-induced AMPA receptor trafficking. *Journal of Neuroscience*, 32(34), 11618-11630.

62. Johnston, M. V., Fatemi, A., Wilson, M. A., & Northington, F. (2011). Treatment advances in neonatal neuroprotection and neurointensive care. *The Lancet Neurology*, 10(4), 372-382.

63. Johnston, M. V., Ishida, A., Ishida, W. N., Matsushita, H. B., Nishimura, A., & Tsuji, M. (2009). Plasticity and injury in the developing brain. *Brain and Development*, 31(1), 1-10.

64. Khan, A., & Rayner, G. D. (2003). Robustness to non-normality of common tests for the many-sample location problem. *Advances in Decision Sciences*, 7(4), 187-206.

65. Kernan, W. N., Ovbiagele, B., Black, H. R., Bravata, D. M., Chimowitz, M. I., Ezekowitz, M. D., Fang, M. C., Fisher, M., Furie, K. L., Heck D.V., Johnston S.C.C., Kasner, S.E., Kittner, S. J., Mitchell, P.H., Rich, M.W., Richardson, D., Schwamm, L.H., Wilson, J.A. (2014). Guidelines for the prevention of stroke in patients with stroke and transient ischemic attack. *Stroke.*, 45(7), 2160-2236.

66. Kim, D. Y., Kim, S. H., Choi, H. B., Min, C. K., & Gwag, B. J. (2001). High abundance of GluR1 mRNA and reduced Q/R editing of GluR2 mRNA in individual NADPH-diaphorase neurons. *Molecular and Cellular Neuroscience,* 17(6), 1025-1033.

67. Kim, T. H., & Vemuganti, R. (2015). Effect of sex and age interactions on functional outcome after stroke. *CNS neuroscience & therapeutics*, 21(4), 327-336.

68. Kirichok, Y., Krapivinsky, G., & Clapham, D. E. (2004). The mitochondrial calcium uniporter is a highly selective ion channel. *Nature*, 427(6972), 360.

69. Koszegi, Z., Fiuza, M., & Hanley, J. G. (2017). Endocytosis and lysosomal degradation of GluA2/3 AMPARs in response to oxygen/glucose deprivation in hippocampal but not cortical neurons. *Scientific reports*, 7(1), 12318.

70. Krueger, H., Koot, J., Hall, R. E., O'Callaghan, C., Bayley, M., & Corbett, D. (2015). Prevalence of Individuals Experiencing the Effects of Stroke in Canada. *Stroke*, 46(8), 2226-2231.

71. Kwak, S. K., & Kim, J. H. (2017). Statistical data preparation: management of missing values and outliers. *Korean journal of anesthesiology*, 70(4), 407.

72. Lakens, D. (2013). Calculating and reporting effect sizes to facilitate cumulative science: a practical primer for t-tests and ANOVAs. *Frontiers in psychology*, 4, 863.

73. Lalonde, C. C., & Mielke, J. G. (2014). Selective vulnerability of hippocampal sub-fields to oxygen–glucose deprivation is a function of animal age. *Brain Research*, *1543*, 271-279.

74. Lau, A., & Tymianski, M. (2010). Glutamate receptors, neurotoxicity and neurodegeneration. *Pflügers Archiv-European Journal of Physiology*, 460(2), 525-542.

75. Li, F., Tan, J., Zhou, F., Hu, Z., & Yang, B. (2018). Heat Shock Protein B8 (HSPB8) Reduces Oxygen-Glucose Deprivation/Reperfusion Injury via the Induction of Mitophagy. *Cellular Physiology and Biochemistry*, 48(4), 1492-1504.

76. Liu, B., Liao, M., Mielke, J. G., Ning, K., Chen, Y., Li, L., ... & Wan, Q. (2006). Ischemic insults direct glutamate receptor subunit 2-lacking AMPA receptors to synaptic sites. *Journal of Neuroscience*, 26(20), 5309-5319.

77. Liu, X. B., Murray, K. D., & Jones, E. G. (2004). Switching of NMDA receptor 2A and 2B subunits at thalamic and cortical synapses during early postnatal development. *Journal of Neuroscience*, 24(40), 8885-8895. 99.

78. Liu M., Dziennis S., Hurn P.D., Alkayed N.J. (2009). Mechanisms of gender-linked ischemic brain injury. *Restor Neurol Neurosci.* 27(3): 163-179.

79. Lu, W., & Roche, K. W. (2012). Posttranslational regulation of AMPA receptor trafficking and function. *Current Opinion in Neurobiology*, 22(3), 470-479.

80. Lu, W., Shi, Y., Jackson, A. C., Bjorgan, K., During, M. J., Sprengel, R. & Nicoll, R. A. (2009). Subunit composition of synaptic AMPA receptors revealed by a single-cell genetic approach. *Neuron*, 62(2), 254-268.

81. Malenka, R. C. (2003). Synaptic plasticity and AMPA receptor trafficking. *Annals of the New York Academy of Sciences*, 1003(1), 1-11.

82. Man, H. Y. (2011). GluA2-lacking, calcium-permeable AMPA receptors—inducers of plasticity?. *Current Opinion in Neurobiology*, 21(2), 291-298.

83. Manwani, B., & McCullough, L. D. (2011). Sexual dimorphism in ischemic stroke: lessons from the laboratory. *Women's Health*, 7(3), 319-339.

84. McCullough, L. D., Zeng, Z., Blizzard, K. K., Debchoudhury, I., & Hurn, P. D. (2005). Ischemic nitric oxide and poly (ADP-ribose) polymerase-1 in cerebral ischemia: male toxicity, female protection. *Journal of Cerebral Blood Flow & Metabolism*, 25(4), 502-512.

85. McIlwain, D. R., Berger, T., & Mak, T. W. (2013). Caspase functions in cell death and disease. *Cold Spring Harbor Perspectives in Biology*, 5(4)

86. Mendis, S., Puska, P., & Norrving, B. (2011). Global atlas on cardiovascular disease prevention

and control. *World Health Organization.*

87. Mergenthaler, P., Dirnagl, U., & Meisel, A. (2004). Pathophysiology of stroke: lessons from animal models. *Metabolic Brain Disease*, 19(3-4), 151-167.

88. Mergenthaler, P., Lindauer, U., Dienel, G. A., & Meisel, A. (2013). Sugar for the brain: the role of glucose in physiological and pathological brain function. *Trends in Neurosciences*, 36(10), 587-597.

89. Mielke, J. G., Comas, T., Ahuja, T., Preston, E., & Mealing, G. A. (2007). Synaptic activity and triphenyltetrazolium chloride metabolism are correlated after oxygen–glucose deprivation in acute, but not cultured, hippocampal slices. *Brain research*, 1176, 113-123.

90. Montori, S., Dos_Anjos, S., Ríos-Granja, M. A., Pérez-García, C. C., Fernández-López, A., & Martínez-Villayandre, B. (2010). AMPA receptor downregulation induced by ischaemia/reperfusion is attenuated by age and blocked by meloxicam. *Neuropathology and applied neurobiology*, 36(5), 436-447.

91. Moser, M. B., Moser, E. I., Forrest, E., Andersen, P., & Morris, R. G. (1995). Spatial learning with a minislab in the dorsal hippocampus. *Proceedings of the National Academy of Sciences*, 92(21), 9697-9701.

92. Mosteller, F., & Tukey, J. W. (1977). Data analysis and regression: a second course in statistics. *Addison-Wesley Series in Behavioral Science: Quantitative Methods.*

93. National Institute of Neurological Disorders and Stroke rt-PA Stroke Study Group. (1995). Tissue plasminogen activator for acute ischemic stroke. *New England Journal of Medicine*, 333(24), 1581-1588.

94. Nguyen, H. B., Bagot, R. C., Diorio, J., Wong, T. P., & Meaney, M. J. (2015). Maternal care differentially affects neuronal excitability and synaptic plasticity in the dorsal and ventral hippocampus. *Neuropsychopharmacology*, 40(7), 1590.

95. Odden, M. C., Pletcher, M. J., Coxson, P. G., Thekkethala, D., Guzman, D., Heller, D., Glodman, L., Bibbins-Domingo, K. (2015). Cost-Effectiveness and Population Impact of Statins for Primary Prevention in Adults Aged 75 Years or Older in the United StatesStatins for Primary Prevention in US Adults Aged 75 Years or Older. *Annals of Internal Medicine*, 162(8), 533-541.

96. Ontario stroke network. (2016). Stroke Stats & Facts. [online] Available at: https://ontariostrokenetwork.ca/information-about-stroke/stroke-stats-and-facts [Accessed 22 July. 2017].

97. Onufriev, M. V., Freiman, S. V., Moiseeva, Y. V., Stepanichev, M. Y., Lazareva, N. A., & Gulyaeva, N. V. (2017). Accumulation of corticosterone and interleukin-1β in the hippocampus after focal ischemic damage of the neocortex: Selective vulnerability of the ventral hippocampus. *Neurochemical Journal*, 11(3), 236-241.

98. Paciaroni, M., Caso, V., & Agnelli, G. (2009). The concept of ischemic penumbra in acute stroke and therapeutic opportunities. *European neurology*, 61(6), 321-330.

99. Paoletti, P., Bellone, C., & Zhou, Q. (2013). NMDA receptor subunit diversity: impact on receptor properties, synaptic plasticity and disease. *Nature Reviews. Neuroscience*, 14(6), 383.

100. Papatheodoropoulos, C., & Kostopoulos, G. (2000). Dorsal-ventral differentiation of short-term synaptic plasticity in rat CA1 hippocampal region. *Neuroscience letters*, 286(1), 57-60.

101. Paxinos, G., & Watson, C. (2017). *The Rat Brain in Stereotaxic Coordinates: Compact 7th Edition.* Academic press.

102. Pellegrini-Giampietro, D. E., Gorter, J. A., Bennett, M. V., & Zukin, R. S. (1997). The GluR2 (GluR-B) hypothesis: Ca2+-permeable AMPA receptors in neurological disorders. *Trends in neurosciences*, 20(10), 464-470.

103. Pollet, T. V., & van der Meij, L. (2017). To remove or not to remove: the impact of outlier handling on significance testing in testosterone data. *Adaptive Human Behavior and Physiology*, 3(1), 43-60.

104. Powers, W. J., Rabinstein, A. A., Ackerson, T., Adeoye, O. M., Bambakidis, N. C., Becker, K., Biller, J., Brown, M., Demaerschalk, B. M., Hoh, B., Jauch, E. C., Kidwell, C. S., Leslie-Mazwi, T. M., Ovbiagele, B., Scott, P. A., Sheth, K. M., Southerland, A. M., Summers, D. V. & Tirschwell, D. L. (2018). 2018 guidelines for the early management of patients with acute ischemic stroke: a guideline for healthcare professionals from the American Heart Association/American Stroke Association. *Stroke*, 49(3), e46-e99.

105. Preston, E., & Webster, J. (2000). Spectrophotometric measurement of experimental brain injury. *Journal of Neuroscience Methods*, *94*(2), 187-192.

106. Rami, A., Ausmeir, F., Winckler, J., & Krieglstein, J. (1997). Differential effects of scopolamine on neuronal survival in ischemia and glutamate neurotoxicity: relationships to the excessive vulnerability of the dorsoseptal hippocampus. *Journal of Chemical Neuroanatomy*, 13(3), 201-208.

107. Reeves, M. J., Bushnell, C. D., Howard, G., Gargano, J. W., Duncan, P. W., Lynch, G., Khatiwoda, A., & Lisabeth, L. (2008). Sex differences in stroke: epidemiology, clinical presentation, medical care, and outcomes. *The Lancet Neurology*, 7(10), 915-926.

108. Sacks, D., Black, C. M., Cognard, C., Connors III, J. J., Frei, D., Gupta, R. & Ramee, S. (2013). Multisociety consensus quality improvement guidelines for intraarterial catheter-directed treatment of acute ischemic stroke, from the american society of neuroradiology, canadian interventional radiology association, cardiovascular and interventional radiological society of europe, society for cardiovascular angiography and interventions, society of interventional radiology, society of neurointerventional surgery, european society of minimally invasive neurological therapy, and society of vascular. *Journal of Vascular and Interventional Radiology*, 24(2), 151-163.

109. Scheiner-Bobis, G. (2002). The sodium pump. *The FEBS Journal*, 269(10), 2424-2433.

110. Schiattarella, G. G., Perrino, C., Magliulo, F., Ilardi, F., Serino, F., Trimarco, V., Izzo, R., Amato, B., Terranova, C., Cardin, F., Militello, C., Leosco, D., Trimarco, B., & Esposito, G.

(2012). Statins and the elderly: recent evidence and current indications. *Aging Clin Exp Res*, 24(3 Suppl), 47-55.

111. Schmidt-Kastner, R., & Freund, T. F. (1991). Selective vulnerability of the hippocampus in brain ischemia. *Neuroscience*, 40(3), 599-636.

112. Schwab, B. L., Guerini, D., Didszun, C., Bano, D., Ferrando-May, E., Fava, E., Tam, J., Xu, D., Xanthoudakis, S., Nicholson, D.W., & Carafoli, E. (2002). Cleavage of plasma membrane calcium pumps by caspases: a link between apoptosis and necrosis. *Cell Death and Differentiation*, 9(8), 818-831.

113. Scott, D., Blizzard, L., Fell, J., & Jones, G. (2009). Statin therapy, muscle function and falls risk in community-dwelling older adults. *QJM: An International Journal of Medicine*, 102(9), 625-633.

114. Siegelbaum, S. A., & Hudspeth, A. J. (2000). *Principles of neural science* (Vol. 4, pp. 324). New York: McGraw-hill.

115. Siesjö, B. K. (1992). Pathophysiology and treatment of focal cerebral ischemia: Part II: mechanisms of damage and treatment. *Journal of neurosurgery*, 77(3), 337-354.

116. Siesjö, B. K., Katsura, K. I., Zhao, Q. I., Folbergraova, J., Pahlmark, K., SIESJÖ, P., & Smith, M. L. (1995). Mechanisms of secondary brain damage in global and focal ischemia: a speculative synthesis. *Journal of neurotrauma*, 12(5), 943-956.

117. Smith, M.L., Auer, R.N. and Siesjö, B.K., The density and distribution of ischemic brain injury in the rat following 2-10 min of forebrain ischemia, *Acta Neuropathol*, 64 (1984a) 319-332.

118. Strange, B. A., Witter, M. P., Lein, E. S., & Moser, E. I. (2014). Functional organization of the hippocampal longitudinal axis. Nature Reviews Neuroscience, 15(10), 655-669.

119. Stroke.nih.gov. (2017). NINDS Know Stroke Campaign - *needtoknow*. [online] Available at: https://stroke.nih.gov/materials/needtoknow.htm [Accessed 13 Aug. 2017].

120. Stys, P. K. (1998). Anoxic and ischemic injury of myelinated axons in CNS white matter: from mechanistic concepts to therapeutics. *Journal of Cerebral Blood Flow & Metabolism*, 18(1), 2-25.

121. Szabadkai, G., & Duchen, M. R. (2008). Mitochondria: the hub of cellular Ca2+ signaling. *Physiology*, 23(2), 84-94.

122. Szydlowska, K., & Tymianski, M. (2010). Calcium, ischemia and excitotoxicity. *Cell Calcium*, 47(2), 122-129.

123. Takagi, Y., Takagi, N., Besshoh, S., Miyake-Takagi, K., & Takeo, S. (2003). Transient global ischemia enhances phosphorylation of the GluR1 subunit of the α-amino-3-hydroxy-5-methylisoxazole-4-propionate receptor in the hippocampal CA1 region in rats. *Neuroscience Letters*, 341(1), 33-36.

124. Tanaka, H., Grooms, S. Y., Bennett, M. V., & Zukin, R. S. (2000). The AMPAR subunit GluR2: still front and center-stage. *Brain research*, 886(1-2), 190-207.

125. Taylor, C. T., & Moncada, S. (2010). Nitric oxide, cytochrome C oxidase, and the cellular response to hypoxia. *Arteriosclerosis, Thrombosis, and Vascular Biology*, 30(4), 643-647.

126. Teng, H., Cai, W., Zhou, L., Zhang, J., Liu, Q., Wang, Y., Dai, W., Zhao, M., & Sun, Z. (2010). Evolutionary mode and functional divergence of vertebrate NMDA receptor subunit 2 genes. *PloS One*, 5(10), e13342.

127. Thacker, J. S., Yeung, D., Chambers, P. J., Tupling, A. R., Staines, W. R., & Mielke, J. G. (2019). Single session, high-intensity aerobic exercise fails to affect plasticity-related protein expression in the rat sensorimotor cortex. *Behavioural brain research*, 359, 853-860.

128. Thacker, J. S., Yeung, D. H., Staines, W. R., & Mielke, J. G. (2016). Total protein or high-abundance protein: Which offers the best loading control for Western blotting?. *Analytical biochemistry*, 496, 76-78.

129. Traynelis, S. F., Wollmuth, L. P., McBain, C. J., Menniti, F. S., Vance, K. M., Ogden, K. K., Hansen, K. B., Yuan H., Myers S. J. & Dingledine, R. (2010). Glutamate receptor ion channels: structure, regulation, and function. *Pharmacological reviews*, 62(3), 405-496.

130. Uchida, M., Palmateer, J. M., Herson, P. S., DeVries, A. C., Cheng, J., & Hurn, P. D. (2009). Dose-dependent effects of androgens on outcome after focal cerebral ischemia in adult male mice. *Journal of Cerebral Blood Flow & Metabolism*, 29(8), 1454-1462.

131. Wang, G., Gilbert, J., & Man, H. Y. (2012). AMPA receptor trafficking in homeostatic synaptic plasticity: functional molecules and signaling cascades. *Neural plasticity*, 2012.

132. Weilinger, N. L., Maslieieva, V., Bialecki, J., Sridharan, S. S., Tang, P. L., & Thompson, R. J. (2013). Ionotropic receptors and ion channels in ischemic neuronal death and dysfunction. *Acta Pharmacologica Sinica*, 34(1), 39-48.

133. Wein, T., Lindsay, M. P., Côté, R., Foley, N., Berlingieri, J., Bhogal, S., Bourgoin, A., Buck, B. H., Cox, J., Davidson, D., Dowlatshahi, D., Douketis, J. Falconer, J., Field, T., Gioia, L., Gubitz, G., Habert, J., Jaspers, S., Lum, C., Morse, D. M., Pageau, P., Rafay, M., Rodgerson, A., Semchuk, B., Sharma, M., Shoamanesh, A., Tamayo, A., Smitko, E. & Gladstoneon D. J. (2018). Canadian stroke best practice recommendations: Secondary prevention of stroke, practice guidelines, update 2017. *International Journal of Stroke,* 13(4), 420-443. ,

134. Wenk, G. L., & Barnes, C. A. (2000). Regional changes in the hippocampal density of AMPA and NMDA receptors across the lifespan of the rat. *Brain research*, 885(1), 1-5.

135. Whitney, N. P., Peng, H., Erdmann, N. B., Tian, C., Monaghan, D. T., & Zheng, J. C. (2008). Calcium-permeable AMPA receptors containing Q/R-unedited GluR2 direct human neural progenitor cell differentiation to neurons. *The FASEB Journal*, 22(8), 2888-2900.

136. World Health Organization. (2017). Cardiovascular diseases (CVDs). [online] Available at: http://www.who.int/mediacentre/factsheets/fs317/en/ [Accessed 22 July. 2017].

137. World Health Organization. (2017). Stroke, Cerebrovascular accident. [online] Available at: http://www.emro.who.int/health-topics/stroke-cerebrovascular-accident/index.html [Accessed 7 December, 2017]

138. Wright, A. L., & Vissel, B. (2012). The essential role of AMPA receptor GluR2 subunit RNA editing in the normal and diseased brain. *Frontiers in molecular neuroscience*, 5, 34.

139. Zhang, F., Guo, A., Liu, C., Comb, M., & Hu, B. (2013). Phosphorylation and assembly of

glutamate receptors after brain ischemia. *Stroke*, 44(1), 170-176.

140. Zhang, Q. G., Raz, L., Wang, R., Han, D., De Sevilla, L., Yang, F., Vadlamudi., R.K., & Brann, D. W. (2009). Estrogen attenuates ischemic oxidative damage via an estrogen receptor α-mediated inhibition of NADPH oxidase activation. *Journal of Neuroscience*, 29(44), 13823-13836.

141. Zhang, T. Y., Keown, C. L., Wen, X., Li, J., Vousden, D. A., Anacker, C., Bhattacharyya, U., Ryan, R., Diorio, J., O'Toole, N., Lerch, J. P., Mukamel, E. A., & Meaney, M. J. (2018). Environmental enrichment increases transcriptional and epigenetic differentiation between mouse dorsal and ventral dentate gyrus. *Nature communications*, 9(1), 298.